Slow-roll inflation in the Jordan frame

Mindaugas Karčiauskas● and José Jaime Terente Díaz●
Departamento de Física Teórica and Instituto de Física de Partículas y del Cosmos IPARCOS,
Universidad Complutense de Madrid, E-28040 Madrid, Spain

Inflation models based on scalar-tensor theories of gravity are formulated in the Jordan frame, but are most often analyzed in the Einstein frame. The transformation between the frames is not always desirable. In this work, we formulate slow-roll conditions in the Jordan frame. This is achieved by comparing different background quantities and approximations on the same spatial slice in both frames. We use these approximations to derive simple equations that can be applied to compute inflation model observables in terms of Jordan frame quantities only. Finally, we apply some of the results to analyze generalized induced gravity models and compare them with the latest observations.

I. INTRODUCTION

The use of modified gravity theories to build inflation models is as old as the paradigm of inflation itself [1]. In particular, scalar-tensor theories are very popular stages on which to construct such models [2–8]. Initially the work within these theories was concentrated on finding inflating solutions. It was realized that the scale factor in the Jordan frame does not have to be accelerating to realize inflation [9,10]. This is in contrast to the requirement in the Einstein frame. The Jordan frame is distinguished by the Planck length l_{Pl} being time dependent. Therefore, it is not the scale factor $a(t)$ itself that is required to be accelerating, but the ratio of the scale factor to the Planck length must be accelerating, $[a(t)/l_{\text{Pl}}(t)]^{\cdot\cdot} > 0.$[1]

Since the introduction of those early models, the precision of cosmological measurements increased drastically. It is no longer enough to construct a modified gravity model that solely provides inflation, one needs to make sure that it satisfies tight observational constraints derived from the properties of the primordial curvature perturbation.

Given a model of inflation in the Einstein frame, very simple methods have been developed to compute the properties of the curvature perturbation. These methods provide relations between the evolution of the homogeneous mode and the perturbations. In particular, for single field models of slow-roll inflation, which are the main interest of the current work, those relations can be written as (see, e.g., [11])

$$A_{\text{s}} = \frac{U}{24\pi^2 \epsilon_U}, \tag{1}$$

$$n_{\text{s}} - 1 = 2\eta_U - 6\epsilon_U, \tag{2}$$

$$r = 16\epsilon_U. \tag{3}$$

The quantities on the lhs of the above equations specify spectral properties of the primordial perturbation: the amplitude and the spectral index of scalar perturbations as well as the tensor-to-scalar ratio, respectively. On the rhs, we have only homogeneous quantities related to the shape of the potential U. They are expressed in terms of slow-roll parameters defined by

$$\epsilon_U \equiv \frac{1}{2}\left(\frac{U_{,\varphi}}{U}\right)^2, \tag{4}$$

$$\eta_U \equiv \frac{U_{,\varphi\varphi}}{U}, \tag{5}$$

where φ is the inflaton with the potential $U(\varphi)$ and the subindices ",φ" denote derivatives with respect to the homogeneous field φ.

To compare with observations, these quantities are evaluated at the time when the pivot scale exits the horizon. Typically, this happens in the range of $\hat{N} = 45\text{–}70e$-folds before the end of inflation, depending on the process of reheating [11].[2]

Instead of using "potential slow-roll parameters" ϵ_U and η_U as above, we can write analogous relations in

---

[1]To make this expression concise, the spacetime slicing is assumed in which the lapse function in the Einstein frame is $\hat{\mathcal{N}} = 1$. This is opposite from what is used in the rest of this work.

[2]We use hats to denote geometric quantities in the Einstein frame.

terms of the Hubble-flow functions [12–14]. The latter being defined as

$$\hat{\epsilon}_1 \equiv -\frac{d\hat{H}/d\hat{\tau}}{\hat{H}^2}, \qquad \hat{\epsilon}_{i+1} \equiv \frac{d\hat{\epsilon}_i/d\hat{\tau}}{\hat{\epsilon}_i \hat{H}}, \qquad (6)$$

where $\hat{\tau}$ is the proper time and $\hat{H}$ is the Hubble parameter, both to be defined later.

Observations constrain the first few parameters to be very small at the time the observable Universe exits the horizon, $\hat{\epsilon}_1$, $\hat{\epsilon}_2 \ll 1$ [15]. In this limit and at the lowest order in small parameters, the two sets of these parameters can be related by

$$\hat{\epsilon}_1 \simeq \epsilon_U, \qquad (7)$$

$$\hat{\epsilon}_2 \simeq 4\epsilon_U - 2\eta_U. \qquad (8)$$

We can therefore write Eqs. (1)–(3) also in terms of the Hubble-flow functions. Plugging Eqs. (7) and (8) into Eqs. (1)–(3), the lowest order result is[3]

$$A_s = \frac{U}{24\pi^2\hat{\epsilon}_1}, \qquad (9)$$

$$n_s - 1 = -2\hat{\epsilon}_1 - \hat{\epsilon}_2, \qquad (10)$$

$$r = 16\hat{\epsilon}_1. \qquad (11)$$

The above expressions can be applied to models formulated in the Einstein frame. However, when dealing with inflation models in the context of scalar-tensor theories of gravity, they are usually formulated in the Jordan frame. In that frame, we cannot apply the above results directly. In many cases, this does not present any problems. One can conformally transform the metric and rewrite the same model in the Einstein frame, where the gravitational part of the action reduces to the Einstein-Hilbert form. In this frame, the above results can be readily applied.

However, such a transformation is not always desirable (see, for example, Ref. [17]). One attractive feature of the Jordan frame expressions is that, typically, matter degrees of freedom are minimally coupled to the gravitational ones. The matter Lagrangian takes the standard form, which is familiar from quantum field theories in flat spacetime with constant coupling constants. Once we transform the action into the Einstein frame, the gravitational degrees of freedom get mixed with the matter degrees of freedom and the simple expressions are lost. Moreover, it is sometimes the case that the dynamical analysis of the system is much simpler in the Jordan frame too.

In all those cases, it would be very convenient to have Jordan frame analogous expressions to Eqs. (1)–(3) and (9)–(11) in order to be able to compute inflation observables without ever transforming the model into the Einstein frame. The goal of this work is to derive such relations.

In this paper, we consider only the simplest case: scalar-tensor theories with a single scalar field and the action

$$S = \int d^4x \sqrt{-g}[F(\phi)R + \mathcal{L}(\phi) + \ldots], \qquad (12)$$

where the nonminimal function F is positive and dots represent matter fields. In the current investigation, we assume that matter fields are negligible and do not affect the dynamics in the regime with which we are concerned. One can, of course, construct models where such fields determine the evolution of the system significantly [18]. In addition, such fields do play the crucial role in the process of reheating. However, we are concerned with the dynamics prior to reheating and assume the matter part of the action is such that the inflationary dynamics are solely determined by the scalar field ϕ. Such restrictions are made in order to limit ourselves to a class of models where the conformal transformation can be easily performed, so that our results can be easily checked. We hope to extend the present analysis to more generic setups in the future.

There have already been a number of works that study cosmological perturbations in the Jordan frame [19–23] and study the equivalence between the curvature perturbation in the two frames [24–28]. A frame-independent formulation of some late Universe processes is developed in [18,29–31] and analogous computations related to inflation and its observables in [18,32–34].

Our approach is different from the mentioned references. Instead of computing the curvature perturbation in the Jordan frame and analyzing its relation with the analogous quantities in the Einstein frame, we are only interested in how *homogeneous* quantities, which are needed to compute inflation observables [such as in Eqs. (1)–(3) and (9)–(11)], map from the Einstein frame to the Jordan frame under the conformal transformation. By doing so, we are able to apply observational constraints to models that are formulated and analyzed solely using homogeneous equations in the Jordan frame. Our method allows for a systematic investigation of these issues and generalizes similar analysis done, for example, in Refs. [35–39] and dynamical analysis in Ref. [40].

Whenever discussing modified gravity theories of this type, there is always a question of equivalence of the Einstein and Jordan frames. Although some disagreement remains in regard to systems dominated by the quantum contributions, in regard to our setup, where the classical homogeneous mode dominates over small quantum fluctuations, the equivalence between the frames is well established [26,41,42].[4]

---

[3]The higher order expressions can be found, for example, in [16].

[4]See, however, Ref. [43] for a differing view.

In this work, we use geometrical units where $c = \hbar = m_{\mathrm{Pl}} = 1$, $m_{\mathrm{Pl}} = (8\pi G)^{-1/2}$ and G is Newton's gravitational constant. We also adopt the "mostly positive" signature of the metric.

II. CONFORMAL FRAMES AND THE CONFORMAL TRANSFORMATION

We start by adopting a coordinate time t that is being used to slice the four-dimensional spacetime into the $t = \mathrm{const}$ spacelike hypersurfaces (the foliation of spacetime) [44] such that they coincide with the constant energy density ones. As we are only interested in Friedmann-Lemaître-Robertson-Walker (FLRW) spacetimes, these slices are also homogeneous and isotropic. Otherwise, the choice of t is arbitrary. However, once it is chosen, we keep t fixed.[5]

The proper time τ, on the other hand, depends on the metric, such that

$$\delta\tau = \mathcal{N}\delta t, \tag{13}$$

where $\mathcal{N}$ is the lapse function given by

$$\mathcal{N} \equiv \sqrt{-g^{\mu\nu}\nabla_\mu t \nabla_\nu t}, \tag{14}$$

and $\nabla_\mu t$ is the gradient of t.[6] Furthermore, to simplify expressions, we can fix spatial coordinates such that the shift vector vanishes, as is the standard practice.

With this choice of spacetime slicing and threading, the flat FLRW metric can be written as

$$ds^2 = -\mathcal{N}^2 dt^2 + a^2(t)\delta_{ij}dx^i dx^j. \tag{15}$$

In the rest of the paper, we will use an overdot to denote derivatives with respect to the coordinate time t, for example, $\dot{\phi} \equiv d\phi/dt$. As the spacetime slicing is fixed throughout, we use the same notation for both Einstein and Jordan frame quantities.

One of the roles the metric plays is to define the units of measure [45]. The transformation of the metric results in the transformation of those units. A particular transformation, which is the subject of this work, is the conformal one (or Weyl transformation). It is often denoted by Ω and written as [46]

$$\hat{g}_{\mu\nu}(x) = \Omega^2(x)g_{\mu\nu}(x). \tag{16}$$

It is obvious from Eqs. (14) and (15) that the conformal

transformation rescales the lapse function $\mathcal{N}$ and the spatial metric. However, this does not imply any change in physical observables, only in their interpretation [47,48]. For example, applying the conformal transformation to a FLRW metric, we can map all the dynamical equations into the Universe, which is static. This procedure does not change physical observables such as the redshift. In a static frame, the redshift is caused by the time dependence of particle masses. The relation between the emitted and observed photon wavelengths is exactly the same in both frames.

The natural application that conformal transformation lends to is the scalar-tensor theory of gravity [10]. Most commonly, in these theories one modifies the gravity sector, as compared to general relativity, leaving the matter sector untouched (see, however, [47] for different models). It is said that in this form the model is expressed in the Jordan frame. Such a frame is convenient because the matter sector is minimally coupled to gravity. However, modifications of the gravity sector render Newton's gravitational constant time dependent, which might lead to some counterintuitive behavior.

To avoid such a behavior and possible mistakes associated with it, one can apply Eq. (16) to rewrite the action in a way that the gravity sector of the model is described by the Einstein-Hilbert action. This is called the Einstein frame, where Newton's gravitational constant does not change with time. The price to pay for simplifying the gravity sector of the action in this way is the complication of the matter sector. The latter becomes directly coupled to the new degree of freedom, often in a complicated way. Therefore, the transformation into the Einstein frame is not always desirable. In those cases, one would like to develop methods of computing the relevant observable quantities solely within the Jordan frame. In the following sections, we will derive a method to perform such computations.

III. INFLATION IN THE EINSTEIN FRAME

In this section, we review the general principles of Einstein frame single field inflation with a noncanonical kinetic term. Normally, one would canonically normalize the field before doing the analysis. However, we keep the noncanonical function explicit. Additionally, to simplify the expressions, one would choose such a spacetime slicing that the proper time coincides with the coordinate time. In practice, that means setting the lapse function to $\hat{\mathcal{N}} = 1$. However, to aid our discussion about inflation observables in the Jordan frame, we do not perform any of these simplifications. The complications introduced in this section will pay off in the later ones.

To make the distinction between the frames clearer we use the caret for Einstein frame *geometric* quantities. For example, the Einstein frame FLRW metric in Eq. (15) is written as

---

[5]Eventually we choose the slicing that simplifies the expressions in the Jordan frame.

[6]More precisely, $\nabla_\mu t$ are the coordinate components of the timelike vector field which is the metric dual to the gradient of t, the latter being a 1-form quantity.

$$d\hat{s}^2 = -\hat{\mathcal{N}}^2 dt^2 + \hat{a}^2(t)\delta_{ij}dx^i dx^j. \quad (17)$$

With every constant time hypersurface, one can associate the intrinsic $^3\hat{R}_{\mu\nu}$, as well as the extrinsic $\hat{K}_{\mu\nu}$, curvature tensors. The trace of the latter determines the volume expansion rate [49]

$$\hat{K} = -\frac{1}{\delta\hat{\mathcal{V}}}\frac{d\delta\hat{\mathcal{V}}}{d\hat{\tau}}, \quad (18)$$

where $\hat{K} \equiv \hat{K}^\mu_\mu$, $\hat{\tau}$ is the proper time, and $\delta\hat{\mathcal{V}} \propto \hat{a}^3$ is the proper volume element. However, instead of $\hat{K}$, it is conventional to use the Hubble parameter given by

$$\hat{H} \equiv -\frac{1}{3}\hat{K}. \quad (19)$$

In terms of the coordinate time t, we can write the above expression as

$$\hat{H} = \frac{\dot{\hat{a}}}{\hat{\mathcal{N}}\hat{a}}. \quad (20)$$

Inflation is defined as the period in the history of the Universe when the expansion rate of the spacelike slices is accelerating, that is

$$\frac{d^2\hat{a}}{d\hat{\tau}^2} > 0. \quad (21)$$

We can relate this condition to the time evolution of the Hubble parameter in Eq. (20). If we define the first Hubble-flow function as in Eq. (6), the above condition is equivalent to

$$\hat{\epsilon}_1 < 1. \quad (22)$$

That is, the Hubble parameter must be changing slowly. Once this condition is broken, inflation ends

$$\hat{\epsilon}_{1\,\mathrm{end}} \equiv 1. \quad (23)$$

Observable scales exit the horizon somewhere between $\hat{N} = 45$ and $70e$-folds before the end of inflation [11]. The current constraints on the Hubble-flow functions at horizon exit are $\hat{\epsilon}_{1*} < 0.0052$ (95% C.L.), $\hat{\epsilon}_{2*} = 0.034 \pm 0.008$ (68% C.L.), and $\hat{\epsilon}_{3*} = 0.13^{+0.40}_{-0.45}$ (95% C.L.) [15], where $\hat{\epsilon}_i$ are defined in Eq. (6). That is, all these parameters are much smaller than unity,

$$|\hat{\epsilon}_i|_* \ll 1, \quad (24)$$

where $i = 1, 2, 3$ and the asterisk denotes the moment when cosmological scales exit the horizon. We will use this fact later to approximate many equations.

In the above discussion, we considered only geometric quantities, without any reference to the matter content.

Next, we specify the general action for the single field inflation models, which can be written as

$$S = \int \sqrt{-\hat{g}}\left[\frac{1}{2}\hat{R} - \frac{1}{2}\mathcal{K}(\phi)\hat{g}^{\mu\nu}\partial_\mu\phi\partial_\nu\phi - U(\phi)\right], \quad (25)$$

where $\hat{g} \equiv \det(\hat{g}_{\mu\nu})$, $\hat{R}$ is the Ricci curvature scalar, and $U(\phi)$ is the potential. Variation of the action in Eq. (25) with respect to the field ϕ gives the Klein-Gordon equation

$$\phi'' + 3\hat{H}\phi' + \frac{\mathcal{K}_{,\phi}}{\mathcal{K}}\frac{1}{2}(\phi')^2 + \frac{U_{,\phi}}{\mathcal{K}} = 0, \quad (26)$$

where the primes denote derivatives with respect to the proper time $\hat{\tau}$.

The variation of the same action with respect to the metric tensor leads to the Einstein equation with the energy-momentum tensor given by

$$T_{\mu\nu} = \mathcal{K}(\phi)\nabla_\mu\phi\nabla_\nu\phi - g_{\mu\nu}\left[\frac{1}{2}\mathcal{K}(\phi)\nabla_\sigma\phi\nabla^\sigma\phi + U(\phi)\right]. \quad (27)$$

From the above expression follows that the energy density and pressure of the scalar field can be written as

$$\rho = -T^0_0 = \frac{1}{2}\mathcal{K}\phi'^2 + U(\phi), \quad (28)$$

$$P = \frac{1}{3}T^i_i = \frac{1}{2}\mathcal{K}\phi'^2 - U(\phi). \quad (29)$$

Taking the "00" and "ii" components of the Einstein equation, one arrives at Friedmann equations

$$\hat{H}^2 = \frac{\frac{1}{2}\mathcal{K}\phi'^2 + U(\phi)}{3}, \quad (30)$$

$$\hat{H}' = -\frac{1}{2}\mathcal{K}\phi'^2, \quad (31)$$

where we used the expressions for ρ and P given in Eqs. (28) and (29), respectively.

Using the conditions in Eq. (24) and the equation of motion in Eq. (26) it is easy to show that Eqs. (30) and (31) imply[7]

---

[7]The condition $|\hat{\epsilon}_2| \ll 1$ implies

$$\left|\frac{\phi''}{\phi'\hat{H}} + \frac{1}{2}\frac{\mathcal{K}_{,\phi}}{\mathcal{K}}\frac{\phi'}{\hat{H}}\right| \ll 1,$$

and Eq. (26) can be written as

$$-\left(\frac{\phi''}{\hat{H}\phi'} + \frac{\mathcal{K}_{,\phi}\phi'}{2\mathcal{K}\hat{H}}\right) = 3 + \frac{U_{,\phi}}{\hat{H}\phi'\mathcal{K}}.$$

The result in Eq. (33) follows from these two relations above.

$$\frac{1}{2}\mathcal{K}\phi'^2 \ll U(\phi), \qquad (32)$$

$$\left|\frac{\phi''}{\phi'\hat{H}} + \frac{\mathcal{K}_{,\phi}}{2\mathcal{K}}\frac{\phi'}{\hat{H}}\right| \ll 3 \simeq \left|\frac{U_{,\phi}}{\hat{H}\mathcal{K}\phi'}\right|. \qquad (33)$$

One can immediately notice from the last expression that, in contrast to the case of the canonically normalized field, $\phi''/(\phi'\hat{H})$ does not have to be small if $\mathcal{K}(\phi)$ is a function that makes the two terms on the lhs in Eq. (33) cancel out.

Applying the above conditions to the Friedman equation (30) we find

$$\hat{H}^2 \simeq \frac{U(\phi)}{3}. \qquad (34)$$

Similarly, the condition in Eq. (33) applied to Eq. (26) yields a simplified equation of motion

$$3\hat{H}\mathcal{K}\phi' \simeq -U_{,\phi}. \qquad (35)$$

Both Eqs. (34) and (35) are called slow-roll equations.

Slow-roll approximation also contains the assumption that the derivative of the above expression holds [11]. This leads to the expression

$$\frac{\phi''}{\hat{H}\phi'} + \frac{\mathcal{K}_{,\phi}}{2\mathcal{K}}\frac{\phi'}{\hat{H}} \simeq \frac{1}{\mathcal{K}}\left[\frac{1}{2}\left(\frac{U_{,\phi}}{U}\right)^2 + \frac{\mathcal{K}_{,\phi}}{2\mathcal{K}}\frac{U_{,\phi}}{U} - \frac{U_{,\phi\phi}}{U}\right], \qquad (36)$$

where the condition in Eq. (32) was applied to the Friedmann equation (30).

As one can see from Eq. (33), the slow-roll condition implies that the rhs of (36) is small. This can be conveniently expressed using slow-roll parameters defined as

$$\epsilon_U \equiv \frac{1}{2\mathcal{K}}\left(\frac{U_{,\phi}}{U}\right)^2, \qquad (37)$$

$$\eta_U \equiv \frac{1}{\mathcal{K}}\left(\frac{U_{,\phi\phi}}{U} - \frac{\mathcal{K}_{,\phi}}{2\mathcal{K}}\frac{U_{,\phi}}{U}\right). \qquad (38)$$

The above definitions are equivalent to the definitions in Eqs. (4) and (5). This can be easily confirmed if we canonically normalize the field, such that $d\varphi \equiv \sqrt{\mathcal{K}}d\phi$. The normalization leads to slow-roll parameters as they are written in those equations.

The slow-roll relations in Eqs. (34) and (35) and the condition in Eq. (32) lead to

$$\epsilon_U \ll 1. \qquad (39)$$

Similarly, applying the condition in Eq. (33) to the expression in Eq. (36) we find

$$|\eta_U| \ll 1. \qquad (40)$$

Notice that the second condition does not necessarily imply $|U_{,\phi\phi}|/U \ll 1$, as would be the case if the derivatives are taken with respect to the canonically normalized field. The terms in the parentheses of Eq. (38) can approximately cancel out, even if each of them is not small separately.

Using the slow-roll equation of motion in Eq. (35) and the approximate Hubble parameter in Eq. (34) we can readily show that

$$\hat{\epsilon}_1 \simeq \epsilon_U. \qquad (41)$$

For later use, it is convenient to rewrite all of the above expressions in terms of the coordinate time t. For example, taking $\delta\hat{\tau} = \hat{\mathcal{N}}\delta t$, the formulas for the Hubble-flow parameters in Eq. (6) become

$$\hat{\epsilon}_1 = -\frac{\dot{\hat{H}}}{\hat{\mathcal{N}}\hat{H}^2}, \qquad (42)$$

$$\hat{\epsilon}_{i+1} = \frac{\dot{\hat{\epsilon}}_i}{\hat{\mathcal{N}}\hat{H}\hat{\epsilon}_i}, \qquad (43)$$

the scalar field equation of motion (26) transforms to

$$\ddot{\phi} + \left(3\frac{\dot{\hat{a}}}{\hat{a}} - \frac{\dot{\hat{\mathcal{N}}}}{\hat{\mathcal{N}}}\right)\dot{\phi} + \frac{\mathcal{K}_{,\phi}}{2\mathcal{K}}\dot{\phi}^2 + \hat{\mathcal{N}}^2\frac{U_{,\phi}}{\mathcal{K}} = 0, \qquad (44)$$

and the Friedman and continuity equations (30) and (31) can be written as

$$\left(\frac{\dot{\hat{a}}}{\hat{a}}\right)^2 = \frac{\frac{1}{2}\mathcal{K}\dot{\phi}^2 + \hat{\mathcal{N}}^2 U(\phi)}{3}, \qquad (45)$$

$$\left(\frac{\dot{\hat{a}}}{\hat{a}}\right)^{\cdot} = \frac{\dot{\hat{\mathcal{N}}}}{\hat{\mathcal{N}}}\frac{\dot{\hat{a}}}{\hat{a}} - \frac{1}{2}\mathcal{K}\dot{\phi}^2. \qquad (46)$$

Notice that $\dot{\hat{a}}/\hat{a}$ is not equal to the Hubble parameter, as the derivative is taken with respect to the coordinate time t and not the proper time $\hat{\tau}$.

Similarly, we can rewrite the slow-roll conditions in Eqs. (32) and (33) as

$$\frac{1}{2}\mathcal{K}(\phi)\dot{\phi}^2 \ll \hat{\mathcal{N}}^2 U(\phi), \qquad (47)$$

$$\frac{1}{2\hat{H}\mathcal{K}\dot{\phi}^2}\left|\frac{d}{dt}\left(\frac{\mathcal{K}\dot{\phi}^2}{\hat{\mathcal{N}}^2}\right)\right| \ll \frac{3}{\hat{\mathcal{N}}} \simeq \left|\frac{U_{,\phi}}{\hat{H}\mathcal{K}\dot{\phi}}\right|. \qquad (48)$$

If these conditions are satisfied, the slow-roll approximate dynamical equations (34) and (35) are given by

$$3\frac{\dot{\hat{a}}}{\hat{a}}\dot{\phi} \simeq -\frac{\hat{\mathcal{N}}^2 U_{,\phi}}{\mathcal{K}}, \qquad (49)$$

$$\left(\frac{\dot{\hat{a}}}{\hat{a}}\right)^2 \simeq \frac{\hat{\mathcal{N}}^2 U(\phi)}{3}. \tag{50}$$

The other utility of slow-roll parameters is that they enable us to write the observable inflation parameters in such a compact form as in Eqs. (1)–(3). However, to compute numerical values of those expressions, we are missing one more component. Equations (1)–(3) are supposed to be evaluated at the time when observable scales (or the pivot scale, more precisely) exit the horizon. The exact time when this happens depends on the specifics of the reheating scenario. For the purpose of this work, the precise value is not important. However, for concreteness, when comparing our results with observations, we will take that to be $\hat{N} = 50$–60 e-folds before the end of inflation, in line with the choice of the Planck team [15].

The number of e-folds of inflation $\hat{N}$ is defined as

$$\hat{N} \equiv \ln \frac{\hat{a}_{\text{end}}}{\hat{a}} = \int\limits_{t}^{t_{\text{end}}} \hat{\mathcal{N}} \, \hat{H} \, dt, \tag{51}$$

where values with the label "end" correspond to the end of inflation, the latter being defined in Eq. (23). Within the slow-roll approximation, this formula can be simplified as

$$\hat{N} \simeq \int\limits_{\phi_{\text{end}}}^{\phi} \sqrt{\frac{\mathcal{K}}{2\epsilon_U}} \, d\phi. \tag{52}$$

Therefore, the computation of inflation observables (at least for these simple models) can be summarized as follows. First, using (52), compute the value of the inflaton ϕ_* that corresponds to a given number of e-folds before the end of inflation. Once ϕ_* is known, it is very easy to compute $U(\phi_*)$, $\epsilon_U(\phi_*)$, and $\eta_U(\phi_*)$ (and higher order parameters if needed). Then, plugging this result into Eqs. (1)–(3), we get numerical values of inflation observables that can be compared with observational constraints.

IV. INFLATION IN SCALAR-TENSOR THEORIES

Having summarized the procedure of computing the observables of slow-roll inflation in the Einstein frame, we next discuss a method of performing the same computation in the Jordan frame.

A. The exact expressions in the Jordan frame

Consider a typical action used in the scalar-tensor theories of gravity,

$$S = \int d^4x \sqrt{-g} \left[\frac{1}{2} F(\phi) R - \frac{1}{2} g^{\mu\nu} \partial_\mu \phi \partial_\nu \phi - V(\phi) \right]. \tag{53}$$

This action also includes models where the scalar field ϕ has a noncanonical kinetic term. This can be shown by performing a field redefinition $\chi \equiv F(\phi)$. Defining $\omega(\chi) \equiv F/(F_\phi)^2$ leads to

$$S = \int d^4x \sqrt{-g} \left[\frac{1}{2} \chi R - \frac{\omega(\chi)}{2\chi} g^{\mu\nu} \partial_\mu \chi \partial_\nu \chi - V(\chi) \right]. \tag{54}$$

By setting $\omega = \text{const}$, which corresponds to $F \propto \phi^2$, and $V(\chi) = 0$ one obtains the Brans-Dicke action [50,51]. For the rest of the paper, we will only use the form of the action in Eq. (53).

As in the previous section, we are only interested in the homogeneous, flat FLRW spacetime. However, in contrast to that section, now we do fix the spacetime slicing. Constant time hypersurfaces are chosen such that the coordinate time equals the proper time in the Jordan frame. That is, in this frame we can write the metric as

$$ds^2 = -dt^2 + a^2(t)\delta_{ij}dx_i dx_j, \tag{55}$$

where the lapse function $\mathcal{N} = 1$.

Next, we can define analogous geometric quantities as in Sec. III. The Hubble parameter is given by the trace of the extrinsic curvature as in Eq. (19) (this time without the hats),

$$H = \frac{\dot{a}}{a}. \tag{56}$$

The dynamical equations can be derived in two ways. One way is to vary the action with respect to the field and its derivative. The Euler equation then leads to the equation of motion for the ϕ field. Varying the same action with respect to the metric leads to the gravitational equations, which can be used to find the Friedman equations.

On the other hand, one can arrive at the same result by using the expressions in Sec. III. To do that, notice that the action in Eq. (53) is transformed into the Einstein frame by plugging $\Omega = \sqrt{F}$ into Eq. (16). This leads to the action in Eq. (25) where the kinetic function and the potential are equal to

$$\mathcal{K}(\phi) = \frac{1}{F} + \frac{3}{2} \left(\frac{F_{,\phi}}{F} \right)^2, \tag{57}$$

and

$$U(\phi) = \frac{V(\phi)}{F^2}, \tag{58}$$

respectively. As we keep the spacetime slicing fixed even when changing the frame, the lapse function and the scale factor in the Einstein frame are functions of F,

$$\hat{\mathcal{N}} = \sqrt{F}, \tag{59}$$

$$\hat{a} = \sqrt{F}a, \tag{60}$$

where $a(t)$ and $\hat{a}(t)$ are Jordan and Einstein frame scale factors respectively [see Eqs. (55) and (17)]. Plugging these expressions into Eqs. (26), (45), and (46) leads to the equation of motion, Friedman equation, and the continuity equation in terms of Jordan frame quantities, respectively,

$$\ddot{\phi} + 3H\dot{\phi} + V_{,\phi} = 3F_{,\phi}(2H^2 + \dot{H}), \tag{61}$$

and

$$H^2 = \frac{\frac{1}{2}\dot{\phi}^2 + V - 3H\dot{F}}{3F}, \tag{62}$$

$$\dot{H} = -\frac{\dot{\phi}^2 - H\dot{F} + \ddot{F}}{2F}. \tag{63}$$

Note, that due to the forcing term on the rhs of Eq. (61) we can no longer assume that starting from initial conditions at rest the field always rolls down toward the minimum of the potential V. In contrast to the Einstein frame intuition, the field can also climb up the potential. It is straightforward to understand this behavior, if we look at the Einstein frame potential in Eq. (58). Taking the derivative with respect to ϕ, we find

$$U_{,\phi} = U\left(\frac{V_{,\phi}}{V} - 2\frac{F_{,\phi}}{F}\right). \tag{64}$$

The gradient of U determines the direction of the gravitational force. The Jordan frame potential V does not have the same significance, and the gravitational force is not uniquely determined by the gradient of V. Depending on the gradient of F, the gravitational force can be directed in the uphill direction of V. This is due to Newton's gravitational "constant" being the function of the field ϕ.[8]

B. Slow-roll approximations

The advantage of computing Jordan frame relations by the above procedure is that the same substitutions can be used to find unambiguously slow-roll conditions and equations in this frame.

To discuss slow-roll inflation, we found it to be of great use to introduce the following set of parameters. First, similar to the Einstein frame Hubble-flow parameters, we introduce analogous ones in the Jordan frame,

$$\epsilon_1 \equiv -\frac{\dot{H}}{H^2}, \qquad \epsilon_{i+1} \equiv \frac{\dot{\epsilon}_i}{\epsilon_i H}. \tag{65}$$

---

[8]See Ref. [52] for a similar discussion.

The time evolution of the nonminimal function F can be also conveniently parametrized by the following hierarchy of parameters:

$$\theta_1 \equiv \frac{\dot{F}}{2HF}, \qquad \theta_{i+1} \equiv \frac{\dot{\theta}_i}{H\theta_i}. \tag{66}$$

In principle, these two sets of parameters are sufficient to describe the system. However, we find that equations are more compact and slow-roll approximations are made clearer if we trade Hubble-flow parameters ϵ_i in favor of γ_i defined as

$$\gamma^2 \equiv \frac{\mathcal{K}\dot{\phi}^2}{2H^2}, \qquad \gamma_{i+1} \equiv \frac{\dot{\gamma}_i}{H\gamma_i}, \tag{67}$$

where $\gamma_1 \equiv \gamma$ and $\mathcal{K}$ is defined in Eq. (57). One can readily demonstrate the relation between the three sets to be

$$\gamma^2 = (\epsilon_1 + \theta_1)(1 + \theta_1) - \theta_1\theta_2, \tag{68}$$

at the lowest order. Taking time derivatives would give relations between higher order parameters. For convenience, we call these three sets the Jordan frame flow parameters. As demonstrated below, ϵ_1, θ_1, and γ^2 all have to be small in slow roll.

Let us first consider the Hubble-flow parameter in Eq. (42) and the condition for inflation in Eq. (22). Plugging first Eqs. (59) and (60) into Eq. (20), we find

$$\hat{H} = \frac{H}{\sqrt{F}}(1 + \theta_1). \tag{69}$$

Taking the time derivative on both sides and plugging the result into Eq. (42), we can express $\hat{\epsilon}_1$ in terms of the Jordan frame quantities

$$\hat{\epsilon}_1 = \frac{\hat{\epsilon}_1 + \theta_1}{1 + \theta_1} - \frac{\theta_1\theta_2}{(1 + \theta_1)^2}. \tag{70}$$

Imposing the bound in Eq. (22) leads to the condition for inflation in the Jordan frame

$$\epsilon_1 < 1 + \frac{\theta_1\theta_2}{1 + \theta_1}. \tag{71}$$

This result demonstrates explicitly a known fact: the Universe can be inflating even if the first Hubble-flow function is larger than unity in the Jordan frame.

To make this point even stronger, we can find the relation between the second time derivative of the scale factor in the two frames,

$$\hat{a}'' = \frac{1}{\sqrt{F}}[\ddot{a}(1 + \theta_1) + aH^2\theta_1\theta_2]. \tag{72}$$

Applying the definition of inflation in Eq. (21) to the above expression, we find

$$\frac{\ddot{a}}{aH^2} > -\frac{\theta_1\theta_2}{1+\theta_1}. \tag{73}$$

In the Einstein frame, the acceleration of the scale factor is the requirement for inflation. However, as can be seen from the above condition, the Jordan frame scale factor does not have to be accelerating in order to have inflation [9,10], as was already mentioned in the Introduction. In other words, even if the acceleration of the Einstein frame scale factor on a given spacetime slice is positive, the acceleration of the Jordan frame scale factor on that same slice can be negative.

The condition in Eq. (71) is the necessary condition for the Universe to be inflating. However, when cosmological scales exit the horizon, observations impose much stronger constraints. Generically, one must fulfil the slow-roll conditions in Eqs. (47) and (48). Plugging Eqs. (57)–(60) into Eq. (47) leads to the first slow-roll relation in the Jordan frame,

$$F\mathcal{K}\dot{\phi}^2 \ll 2V, \tag{74}$$

or equivalently,

$$\gamma^2 \ll \frac{V}{H^2 F}. \tag{75}$$

Plugging, next, those same equations into Eq. (48), we find the second slow-roll relation,

$$\frac{1}{2}\left|\frac{(\mathcal{K}\dot{\phi}^2)^{\bullet}}{\mathcal{K}\dot{\phi}^2} - \frac{\dot{F}}{F}\right| \ll 3\left(\frac{\dot{F}}{2F} + H\right) \simeq \frac{V}{F\mathcal{K}\dot{\phi}^2}\left|\frac{\dot{V}}{V} - 2\frac{\dot{F}}{F}\right|. \tag{76}$$

In terms of the ϵ_1, θ_1, and γ^2 parameters, this condition can also be written as

$$|\gamma_2 - \epsilon_1 - \theta_1| \ll 3(1+\theta_1) \simeq \frac{V}{2H^2 F\gamma^2}\left|\frac{\dot{V}}{HV} - 4\theta_1\right|. \tag{77}$$

The above relations are obtained by the direct mapping of the Einstein frame slow-roll conditions into the Jordan frame. We proceed next to investigate their implications for the Jordan frame dynamical equations.

First, we rewrite Eq. (74) as $\dot{\phi}^2 + \frac{3}{2}\frac{\dot{F}^2}{F} \ll 2V$. As both terms on the lhs of this expression are positive, the condition has to be satisfied for each of the terms separately. That is,

$$\frac{1}{2}\dot{\phi}^2 \ll V, \tag{78}$$

$$\frac{1}{2}\theta_1^2 \ll \frac{V}{3H^2 F}. \tag{79}$$

We can next rewrite the Friedmann equation (62) as

$$1 + 2\theta_1 = \frac{V + \frac{1}{2}\dot{\phi}^2}{3FH^2}. \tag{80}$$

The second term on the rhs of this expression can be dropped due to the slow-roll condition in Eq. (78). And the condition in Eq. (79) leads to

$$\frac{1}{2}\theta_1^2 \ll 1 + 2\theta_1 \simeq \frac{V}{3FH^2}. \tag{81}$$

The inequality can be satisfied only in the case of

$$|\theta_1| \ll 1. \tag{82}$$

Therefore, the slow-roll approximated Friedmann equation in the Jordan frame is given by

$$H^2 \simeq \frac{V}{3F}. \tag{83}$$

To derive the slow-roll equation of motion, we make use of its expression in the Einstein frame in Eq. (49) and use the same substitutions as above. This leads to

$$3H\dot{\phi} \simeq \frac{2VF_{,\phi} - FV_{,\phi}}{F^2\mathcal{K}(1+\theta_1)}, \tag{84}$$

which can be simplified after imposing the slow-roll condition in Eq. (82),

$$3H\dot{\phi} \simeq \frac{2VF_{,\phi} - FV_{,\phi}}{F^2\mathcal{K}}. \tag{85}$$

It is worth noticing here, as is it pointed out in Ref. [39], that one can find a very similar slow-roll expression used in the literature: $3H\dot{\phi} \simeq (2VF_{,\phi} - FV_{,\phi})/F$ (see, for example, Refs. [35,37,38]). It is obtained by applying, what is sometimes called "generalized slow-roll" approximation [35,39,53]. Comparing with Eq. (85), we can see that this expression is equivalent to neglecting the $F_{,\phi}^2/F$ term. However, generally neglecting this term is not justified. As we show in Sec. V, the generalized induced gravity model is compatible with observations only in the region where precisely $F_{,\phi}^2 \gg F$. Moreover, by performing computer simulations, the authors of Ref. [40] demonstrate that, indeed, Eq. (85) is the slow-roll attractor. In Ref. [39], one can find an analysis of some implications resulting from the two different expressions.

Having shown that slow-roll inflation requires the time derivative of F to be small, we can do the same for other functions. First, we make use of the rhs relation of the slow-roll expression in Eq. (77). As θ_1 is slow-roll suppressed and $V/H^2 F\gamma^2 \gg 1$, according to Eq. (75), the relation $3 \simeq (V/2H^2 F\gamma^2)|\dot{V}/HV - 4\theta_1|$ [cf. Eq. (77)] leads to

$$\frac{\dot{V}}{HV} \ll 1. \tag{86}$$

Another set of slow-roll conditions can be found from the lhs of Eq. (77). Neglecting again θ_1, one finds

$$|\gamma_2 - \epsilon_1| \ll 1. \tag{87}$$

By itself, this slow-roll condition does not require either γ_2 or ϵ_1 to be small if they are tuned to cancel out. As we will see shortly, if both of these terms are larger than 1, such a cancellation also requires one more cancellation with a large θ_2 value. To stay generic, we assume no such cancellations and write

$$|\gamma_2| \ll 1, \tag{88}$$

$$|\epsilon_1| \ll 1. \tag{89}$$

To derive other implications of the slow-roll condition, we can use Eqs. (31) and (69) to write

$$\hat{\epsilon}_1 = \frac{\gamma^2}{(1 + \theta_1)^2}. \tag{90}$$

Therefore, applying slow-roll conditions in Eqs. (82) and (24), we find

$$\frac{\dot{\phi}^2}{2H^2 F} \ll 1, \tag{91}$$

and

$$\hat{\epsilon}_1 \simeq \gamma^2. \tag{92}$$

Higher order smallness parameters can be derived by taking higher derivatives of Eq. (92). For example, the second Hubble-flow parameter in the Einstein frame can be related to the Jordan frame flow parameters by

$$\hat{\epsilon}_2 = \frac{2}{1 + \theta_1}\left(\gamma_2 - \frac{\theta_1\theta_2}{1 + \theta_1}\right). \tag{93}$$

Up to the lowest order in θ_1, this expression can be simplified as

$$\hat{\epsilon}_2 \simeq 2(\gamma_2 - \theta_1\theta_2). \tag{94}$$

The above result makes it clear that the slow-roll condition $\hat{\epsilon}_2 \ll 1$ can be satisfied even for large values of $|\gamma_2|$ and $|\theta_1\theta_2|$, if they approximately cancel out. Paired with Eq. (87), this leads to $\gamma_2 \simeq \epsilon_1 \simeq \theta_1\theta_2$. However, we do not analyze this case any further, as mentioned above, and generically write the condition as

$$|\theta_1\theta_2| \ll 1, \tag{95}$$

which still permits $|\theta_2| \sim 1$ for small $|\theta_1|$. Such large $|\theta_2|$ values imply $|\ddot{F}| \sim H|\dot{F}|$, which could provide a counterexample to the approximation $|\ddot{F}| \ll H|\dot{F}|$, which is often used in the literature.

C. Inflation observables in the Jordan frame

In the Einstein frame, we can relate the Hubble-flow parameters with spectral properties of the primordial curvature perturbation as shown in Eqs. (9)–(11). Having derived the relation between Einstein frame Hubble-flow parameters and analogous quantities in the Jordan frame in Eqs. (92) and (94), we can relate them with the spectral properties of the primordial curvature perturbation as

$$A_s \simeq \frac{V}{24\pi^2 F^2 \gamma^2}, \tag{96}$$

$$n_s - 1 \simeq -2(\gamma^2 + \gamma_2 - \theta_1\theta_2), \tag{97}$$

$$r \simeq 16\gamma^2. \tag{98}$$

Instead of using the γ parameter, we can also express the above relations in terms of the Jordan frame Hubble-flow parameters defined in Eq. (65). To do that we first apply slow-roll approximation to Eq. (68), finding

$$\gamma^2 \simeq \epsilon_1 + \theta_1 - \theta_1\theta_2, \tag{99}$$

where we kept the last term because $|\theta_2|$ is allowed to be of order 1 [see Eq. (95)]. Taking the derivative of Eq. (99) and plugging the result into Eqs. (96)–(98), we find

$$A_s \simeq \frac{V}{24\pi^2 F^2 (\epsilon_1 + \theta_1 - \theta_1\theta_2)}, \tag{100}$$

$$n_s - 1 \simeq -2\left(\epsilon_1 + \theta_1 - 2\theta_1\theta_2 + \frac{\epsilon_2\epsilon_1 + \theta_1\theta_2(1 - \theta_2 - \theta_3)}{2(\epsilon_1 + \theta_1 - \theta_1\theta_2)}\right), \tag{101}$$

$$r \simeq 16(\epsilon_1 + \theta_1 - \theta_1\theta_2). \tag{102}$$

The above expressions are consistent with Eqs. (20) in Ref. [39]. However, we do not assume $|\theta_2|, |\theta_3| \ll 1$. These parameters are allowed to be of order 1 by slow-roll approximation as it is argued below Eq. (95).

The above equations relate the observable parameters of slow-roll inflation with Jordan frame quantities. However, these equations are not sufficient to compare them with observations. We need to specify the moment at which they must be evaluated. Within the single field slow-roll models of inflation, it is sufficiently accurate to evaluate the above expressions at the moment when the pivot scale exits the

horizon. In the Einstein frame, this is assumed to happen $\hat{N}_*$ e-folds before the end of inflation. The Planck satellite team considers $\hat{N}_* = 50\text{--}60$. However, the Jordan frame number of e-folds N does not necessarily correspond to the same numerical value as $\hat{N}$ [31,54,55].

We define the number of e-folds N in the Jordan frame analogously to its counterpart in the Einstein frame, which is given in Eq. (51),

$$N \equiv \ln\frac{a_{\rm end}}{a} = \int_t^{t_{\rm end}} H {\rm d}t. \qquad (103)$$

Remember, since we keep the spacetime slicing fixed, the initial slice at t coincides in the Einstein as well as Jordan frames. The same can be said about the $t_{\rm end}$ slice. In other words, the limits of integration are the same in both frames. Plugging Eqs. (59) and (69) into Eq. (51) and using Eq. (103), we get

$${\rm d}\hat{N} = (1 + \theta_1){\rm d}N. \qquad (104)$$

When cosmological scales exit the horizon, $|\theta_1| \ll 1$ according to Eq. (82), making the difference between ${\rm d}\hat{N}$ and ${\rm d}N$ slow-roll suppressed. However, N is an integral quantity. Therefore, depending on the behavior of $|\theta_1|$ throughout inflation, the total e-fold shift number between the Einstein and Jordan frames can become observationally relevant (see the models in Sec. V B, for example). We can readily compute this shift number $\int \theta_1 {\rm d}N$. Using the definition of θ_1 in Eq. (66) and the definition of e-fold numbers in Eq. (103) gives

$$\hat{N} = N + \frac{1}{2}\ln\frac{F_{\rm end}}{F}. \qquad (105)$$

Although in this work we are only concerned about homogeneous quantities (apart from the numerical simulations in the Appendix), we would also like to comment here about the horizon crossing time (see also [31]). In the Einstein frame, a mode of perturbation is said to leave the horizon when its wave number is $k = \hat{a}\hat{H}$ (see, e.g., [11] for details). Using the transformations in Eqs. (69) and (60), we can easily find that this corresponds to

$$\hat{a}\hat{H} = aH(1 + \theta_1). \qquad (106)$$

As we can see, for cosmological scales, where slow-roll conditions are meant to be applicable, the error of the often used choice $k = aH$ is of the order of slow roll [see Eq. (82)].

D. Slow-roll parameters

Equations (96)–(98) are perfectly valid equations to compute inflation observables in the Jordan frame. They

can be considered as analogous equations to the expressions in terms of the Hubble-flow functions in the Einstein frame as in Eqs. (9)–(11). However, the computational benefit of the slow-roll attractor is that time derivatives become unique functions of the field value, provided by slow-roll equation of motion. Therefore, this effectively reduces the dynamical degrees of freedom.

In the Einstein frame, this computational benefit is utilized by writing the inflation observables as functions of the field, as in Eqs. (1)–(3). We can also do the same in the Jordan frame.

First, we can use the relation between Einstein frame Hubble-flow parameters and the Jordan frame parameters in Eqs. (92) and (94). Plugging these into Eqs. (7) and (8), we find

$$\epsilon_U \simeq \hat{\epsilon}_1 \simeq \gamma^2, \qquad (107)$$

$$4\epsilon_U - 2\eta_U \simeq \hat{\epsilon}_2 \simeq 2(\gamma_2 - \theta_1\theta_2). \qquad (108)$$

The consistency of the above result can be checked directly using Eqs. (37) and (38). Plugging in the expression for U in Eq. (58), we arrive at

$$\epsilon_U = \frac{1}{2\mathcal{K}}\left(\frac{V_{,\phi}}{V} - 2\frac{F_{,\phi}}{F}\right)^2. \qquad (109)$$

Using the Jordan frame slow-roll equation of motion (85), slow-roll Friedmann equation (83), and the definition of γ in Eq. (67), we arrive at (107).

As mentioned above, slow-roll approximation also contains the assumption that the time derivative of the slow-roll equation of motion in Eq. (84) holds. This leads to

$$\gamma_2 - \theta_1\theta_2 \simeq \eta_{FV}, \qquad (110)$$

where we defined

$$\eta_{FV} \equiv 2\epsilon_U - \eta_U$$
$$= \frac{1}{\mathcal{K}}\left[2\frac{F_{,\phi\phi}}{F} - \frac{V_{,\phi\phi}}{V} - 2\frac{F_{,\phi}^2}{F^2} + \frac{V_{,\phi}^2}{V^2} + \frac{\mathcal{K}_{,\phi}}{2\mathcal{K}}\left(\frac{V_{,\phi}}{V} - 2\frac{F_{,\phi}}{F}\right)\right],$$
$$(111)$$

which, again, could be derived by directly plugging in the expression for U into the definition of η_U in Eq. (38). Notice that we did not use Eq. (85) to derive the above result, because θ_2 does not necessarily have to be small. That is, $\theta_1\theta_2$ is allowed to be of order slow roll and not slow-roll squared.

According to the slow-roll condition in Eq. (77), the lhs of the above result has to be small, hence the rhs too. It follows then, that we can write the second slow-roll constraint as

$$|\eta_{FV}| \ll 1. \tag{112}$$

This can be equally well confirmed by Eq. (108): $2\eta_{FV} \simeq \hat{\epsilon}_2 \ll 1$.

Plugging Eqs. (107) and (110) into (1)–(3), we arrive at slow-roll expressions that relate inflation observables with functions F and V

$$A_s \simeq \frac{V}{24\pi^2 F^2 \epsilon_U}, \tag{113}$$

$$n_s - 1 \simeq -2(\epsilon_U + \eta_{FV}), \tag{114}$$

$$r \simeq 16\epsilon_U, \tag{115}$$

where ϵ_U is meant to be evaluated using Eq. (109).

We can also conveniently slow-roll approximate the number of e-folds of inflation in the Jordan frame. Using the definition of N in Eq. (103) and slow-roll equation of motion in Eq. (85), we arrive at

$$N \simeq \int_\phi^{\phi_{\text{end}}} \frac{\mathcal{K}}{2\frac{F_{,\phi}}{F} - \frac{V_{,\phi}}{V}} d\phi. \tag{116}$$

So far, we have considered a generic expression for $\mathcal{K}$. However, the definition of $\mathcal{K}$ in Eq. (57) contains two positive terms. These terms remain comparable throughout inflation only for a specific form of F, namely,

$$F = (\alpha\phi + \beta)^2, \tag{117}$$

with $\alpha = \mathcal{O}(1)$. In the case of $\alpha = 1/\sqrt{6}$, both of those terms are equal. More generically, however, one of them should be dominant. In those cases the expressions can be somewhat simplified.

Consider first the case $F_{,\phi}^2 \ll F$. That is, the approximate expression for $\mathcal{K}$ is given by

$$\mathcal{K} \simeq \frac{1}{F}. \tag{118}$$

In this case, the slow-roll equation of motion (85) can be approximated as

$$\frac{\dot{\phi}}{H} \simeq 2F_{,\phi} - F\frac{V_{,\phi}}{V}, \tag{119}$$

and slow-roll parameter ϵ_U as

$$\epsilon_U \simeq \frac{F_{,\phi}^2}{2F}\left(2 - \frac{F}{F_{,\phi}}\frac{V_{,\phi}}{V}\right)^2. \tag{120}$$

The smallness of ϵ_U implies

$$\frac{1}{2}\left(\frac{V_{,\phi}}{V}\right)^2 \ll \frac{1}{F}. \tag{121}$$

The second slow-roll parameter η_{FV} [defined in Eq. (111)] in this approximation can be simplified as

$$\eta_{FV} \simeq 2F_{,\phi\phi} + F\left(\frac{V_{,\phi}^2}{V^2} - \frac{V_{,\phi\phi}}{V} - \frac{F_{,\phi}^2}{F^2} - \frac{F_{,\phi}}{2F}\frac{V_{,\phi}}{V}\right), \tag{122}$$

where we also applied $|F_{,\phi\phi}| \ll 1$. Finally, the number of e-folds in this regime can be expressed as

$$N \simeq \int_{\phi_{\text{end}}}^{\phi} \frac{1}{\frac{V_{,\phi}}{V} - 2\frac{F_{,\phi}}{F}}\frac{d\phi}{F}. \tag{123}$$

In the opposite case, $F_{,\phi}^2 \gg F$ and

$$\mathcal{K} \simeq \frac{3}{2}\frac{F_{,\phi}^2}{F^2}. \tag{124}$$

The slow-roll equation of motion can then be approximated as

$$\frac{\dot{\phi}}{H} \simeq \frac{2}{3}\frac{F}{F_{,\phi}}\left(2 - \frac{F}{F_{,\phi}}\frac{V_{,\phi}}{V}\right), \tag{125}$$

while the slow-roll parameter ϵ_U is given by

$$\epsilon_U \simeq \frac{1}{3}\left(2 - \frac{F}{F_{,\phi}}\frac{V_{,\phi}}{V}\right)^2. \tag{126}$$

We can see that in this regime slow-roll condition $\epsilon_U \ll 1$ requires the cancellation

$$\frac{V_{,\phi}}{V} \simeq 2\frac{F_{,\phi}}{F}, \tag{127}$$

up to slow-roll precision.

The second slow-roll parameter η_{FV} can be simplified as

$$\eta_{FV} \simeq \frac{2F^2}{3F_{,\phi}^2}\left[\frac{V_{,\phi}^2}{V^2} - \frac{V_{,\phi\phi}}{V} + \left(F_{,\phi\phi} - \frac{F_{,\phi}^2}{F}\right)\frac{V_{,\phi}}{F_{,\phi}V}\right]. \tag{128}$$

Finally, the number of e-folds of inflation in the Jordan frame is given by

$$N \simeq \frac{3}{2}\int_{\phi_{\text{end}}}^{\phi} \frac{F_{,\phi}^2/F}{\frac{V_{,\phi}}{V} - 2\frac{F_{,\phi}}{F}}\frac{d\phi}{F}. \tag{129}$$

We can also study separately the case $F_{,\phi}^2 \simeq F$, which leads to Eq. (117). In this case,

$$\epsilon_U \simeq \mathcal{O}(1)\left(2 - \frac{F}{F_{,\phi}}\frac{V_{,\phi}}{V}\right)^2, \qquad (130)$$

and the same condition as in Eq. (127) must be satisfied for slow-roll inflation to be realized.

V. GENERALIZED INDUCED GRAVITY INFLATION

In this section, we analyze an induced gravity model of inflation [5,6,56]. However, we generalize the model by allowing for arbitrary powers of nonminimal function and the spontaneous symmetry breaking potential. We are also going to search for models that are consistent with the current observational constraints of the scalar spectral index and tensor-to-scalar ratio. The main purpose of this exercise is to make use of the equations derived in the previous section.[9]

The generalization of the induced gravity model that we study can be written as

$$F = \xi\phi^p, \qquad (131)$$

$$V = \frac{\lambda}{2q}(\phi^2 - v^2)^q, \qquad (132)$$

where $|p|$ and q are of order 1. In addition, q must be an even, positive number in order for the potential to be bounded from below.[10] The $p = q = 2$ case with $\phi \gg v$ has been studied extensively in the literature (see Refs. [5–7,56,58–64] for some early work on such models). In this section, our goal is to investigate if inflation is possible in a broader range of parameters, where q is not necessarily equal to p and the field ϕ rolls down the potential from both sides of the minimum.

As F must be positive to avoid instabilities, we fix $\xi > 0$. In that case, it will be assumed that for *odd* values of p we are only interested in $\phi > 0$ region.

In these class of models, one further assumes that eventually the ϕ field settles down at the minimum of the potential V with $\phi = v$. At that point, $F = 1$ and we recover the action of general relativity. This requirement leads to the normalization $\xi v^p = 1$. We make use of this relation to simplify the expressions by normalizing the ϕ field as

$$x \equiv \frac{\phi}{v}. \qquad (133)$$

The potential is symmetric under the transformation $\phi \to -\phi$. Therefore, x is positive.[11] Using this definition, Eqs. (131) and (132) can be written as

$$F(x) = x^p, \qquad (134)$$

$$V(x) = \frac{\lambda}{2q\xi^{2q/p}}(x^2 - 1)^q. \qquad (135)$$

In the context of inflation, the regime $x < 1$ corresponds to hilltoplike inflation models and in the regime $x > 1$ one is led to the chaoticlike models. We will use this terminology below to distinguish the two regimes.

Remember, however, that in the Jordan frame the field does not necessarily roll down the potential V; it can as well climb up the potential. Hence, we need to impose additional conditions in order to guarantee that the end point of the evolution is at $x = 1$.

To that aim, let us first write the slow-roll equation of motion (85) for this model. In terms of x, it is given by

$$\frac{\dot{x}}{H} \simeq -\frac{4\xi^{2/p}x^{p-1}}{2 + 3p^2\xi^{2/p}x^{p-2}} \cdot \frac{(q-p)x^2 + p}{x^2 - 1}. \qquad (136)$$

As is discussed in the paragraph containing Eq. (64), the above slow-roll equation does not necessarily describe a field rolling down toward the minimum of the potential $V(x)$. This becomes evident if we take the initial conditions to be $x \ll 1$, which corresponds to the hilltop setup. In order for the field to slow-roll toward $x = 1$, the field velocity must be positive, $\dot{x} > 0$. However, this can be satisfied only in the case with $p > 0$. Otherwise, the field climbs up the potential, away from the $x = 1$ value and toward $x = 0$. In the opposite regime, where $x \gg 1$, the field rolls down the potential if the velocity is negative, $\dot{x} < 0$. Again, this leads to the condition $p > 0$ if $q = p$, or $p < q$ if $q \neq p$. Notice, that in the latter case it is consistent to consider negative values of p.

This behavior becomes obvious if we write the Einstein frame scalar field potential. According to Eq. (64),

$$U_{,x} = 2U\left[\frac{(q-p)x^2 + p}{x(x^2 - 1)}\right]. \qquad (137)$$

We can readily notice that for very small x the force is directed toward the minimum of U only for $p > 0$. While for large x, the same is true either for $p > 0$, in the case of $p = q$, or for $q > p$, in the case of $p \neq q$. These conditions are summarized in the following equation:

---

[9]Recently, some works (see, for example, Refs. [52,57]) have been published that analyze models that overlap with the ones considered in this section in some parameter space. However, our main goal is to derive analytical expressions of the constraints that can be compared with observations.

[10]Unbounded potential V also results in an unbounded potential U in Eq. (58).

[11]If initially $\phi > 0$, then it runs toward the $\phi \to v$ minimum and toward $\phi \to -v$ otherwise.

$$p > 0 \quad \text{if } x \ll 1 \text{ (hilltop models)},$$
$$p \leq q \quad \text{if } x \gg 1 \text{ (chaotic models)}. \tag{138}$$

Before separating the analysis into the hilltop and chaotic type regimes, let us first compute the general expression for the ϵ_U slow-roll parameter. From Eq. (109), we find

$$\epsilon_U \simeq \frac{4p^2 \xi^{2/p} x^{p-2}}{2 + 3p^2 \xi^{2/p} x^{p-2}} \left[\frac{(\frac{q}{p} - 1)x^2 + 1}{x^2 - 1} \right]^2. \tag{139}$$

As we know, the $\epsilon_U \ll 1$ condition serves as a good proxy to indicate the regime where $\hat{\epsilon}_1 \ll 1$ [see Eq. (7)]. The end of inflation is then approximately given by the condition $\epsilon_U \simeq 1$, which we will use in the following computations.

A. Hilltop type models

In this regime, we take the approximation

$$x_* \ll 1, \tag{140}$$

where the asterisk denotes values when cosmological scales exit the horizon. Within this approximation, we can simplify the expression for ϵ_U in Eq. (139) as

$$\epsilon_U \simeq \frac{4p^2 \xi^{2/p} x^{p-2}}{2 + 3p^2 \xi^{2/p} x^{p-2}}. \tag{141}$$

It depends on the value of p if slow-roll inflation can be realized or not. Let us therefore consider first $p > 2$. In this case, ϵ_U monotonically decreases as we decrease x and from Eq. (141) it is clear that to satisfy the $\epsilon_U \ll 1$ condition we need to impose the bound

$$p^2 \xi^{2/p} x^{p-2} \ll 1. \tag{142}$$

Note that from the definition of F in Eq. (131), this condition is equivalent to $F_{,\phi}^2 \ll F$. Therefore, we can use Eq. (122) to compute the second slow-roll parameter η_{FV} as

$$\eta_{FV} \simeq -p(2 - p)\xi^{2/p} x^{p-2}, \tag{143}$$

and approximate Eq. (141) as

$$\epsilon_U \simeq 2p^2 \xi^{2/p} x^{p-2}. \tag{144}$$

Plugging the last two expressions into Eqs. (114) and (115) gives

$$n_s - 1 \simeq \frac{2 - 3p}{16p} r. \tag{145}$$

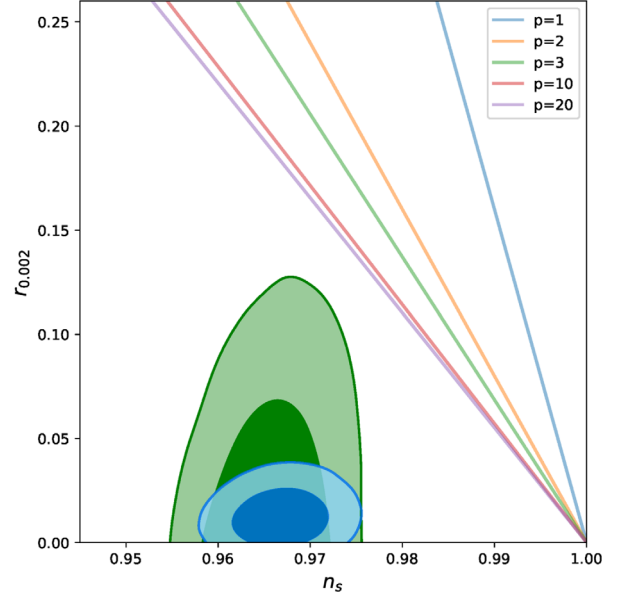As we can see in Fig. 1, these models fall outside the observationally allowed region.

FIG. 1. The comparison of observational constraints on scalar spectral index n_s and the tensor-to-scalar ratio r with predictions of the generalized induced gravity models in the hilltop regime. The green contours represent 1σ and 2σ constraints from Ref. [15] and the blue contours add the new BICEP/Keck observations (see Ref. [65] for details). $p > 0$ is required for hilltop models. Note also that the presence of a line for some values of r vs n_s does not necessarily imply that those values can be actually realized within a given model (which also holds for all the plots below). To establish this one needs to compute the number of e-folds $\hat{N}_*$. As the lines lie outside the observationally allowed region anyway, we did not perform this computation.

The above relation is also applicable for $p = 2$ and $p = 1$ values too. In the former case, $\epsilon_U \simeq \text{const}$ as long as $x \ll 1$ is satisfied. Hence, slow-roll inflation, with $\epsilon_U \ll 1$, is only possible for

$$\xi \ll 1/2. \tag{146}$$

In the case of $p = 1$, the $p^2 \xi^{2/p} x^{p-2}$ term is a decreasing function of x. As we can clearly see from Eq. (141), this implies

$$\epsilon_U \xrightarrow{x \to 0} \frac{4}{3}, \tag{147}$$

which is a noninflationary regime. Hence, the slow-roll inflation can be realized only for field values

$$x \gg \frac{1}{2} \xi^2. \tag{148}$$

Both expressions in Eqs. (146) and (148) imply $F_{,\phi}^2 \ll F$. This justifies using an approximate relation in Eq. (122) to compute η_{FV} and therefore Eq. (145) to
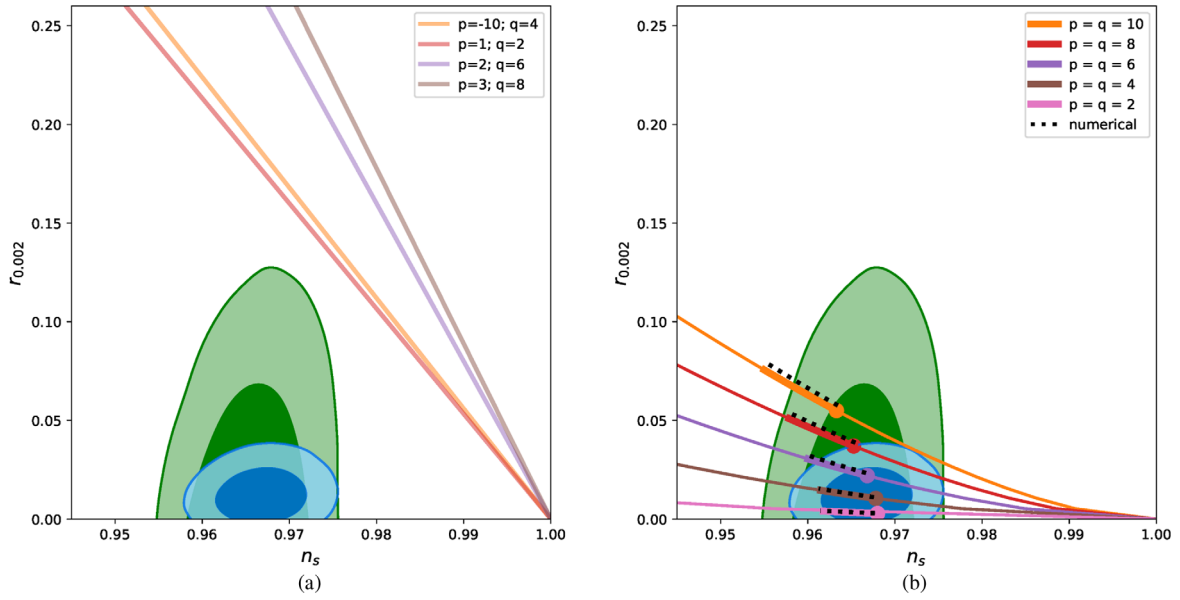
FIG. 2. Comparison of observational constraints of inflationary parameters n_s and r with chaotic type ($x_* \gg 1$) models of generalized induced gravity theories. (a) Models with $p < q$ and $F_{,\phi}^2 \ll F$. (b) Models with $p = q$ and $F_{,\phi}^2 \gg F$. Thick sections of curves show $\hat{N}_* \in [50; 60]$ range, where large points correspond to the $\hat{N}_* = 60$ value. The black dotted curves represent the results from exact numerical simulations (see the Appendix) in the same $\hat{N}_*$ range. The contours are the same as in Fig. 1.

compute $n_s(r)$ relation. Unfortunately, all the hilltop type models lie outside the observationally allowed region.

B. Chaotic type models

We call "chaotic" models that satisfy

$$x_* \gg 1. \qquad (149)$$

The lowest order approximation of ϵ_U in Eq. (139) in terms of x^{-2} depends on the relation between p and q. Let us consider first the case where $p \neq q$. As can be seen in Eq. (138), this case also permits negative values of p and ϵ_U is approximately given by

$$\epsilon_U \simeq \frac{4p^2 \xi^{2/p} x^{p-2}}{2 + 3p^2 \xi^{2/p} x^{p-2}} \left(\frac{q}{p} - 1\right)^2. \qquad (150)$$

In the limit $p^2 \xi^{2/p} x^{p-2} \gg 1$, which is equivalent to $F_{,\phi}^2 \gg F$, the first factor in the above expression is $\sim 4/3$. However, for p and q of order 1, the second factor $(q/p - 1)^2 \sim \mathcal{O}(1)$. Therefore slow-roll inflation can only be realized for models with

$$p^2 \xi^{2/p} x^{p-2} \ll 1. \qquad (151)$$

As this condition is equivalent to $F_{,\phi}^2 \ll F$, we can use an approximate expression of η_{FV} in Eq. (122) again,

$$\eta_{FV} \simeq \begin{cases} qp^2 \xi^{2/p} x^{p-4} & \text{for } p = 2 \\ (q-p)(2-p)\xi^{2/p} x^{p-2} & \text{for } p \neq 2, \end{cases} \qquad (152)$$

to the lowest orders in x^{-2} and $p^2 \xi^{2/p} x^{p-2}$.

We can readily notice that for $x \gg 1$ the slow-roll parameter $\epsilon_U \gg \eta_{FV}$. Therefore, using Eqs. (114) and (115) we can write a unified expression for all values of p as

$$n_s - 1 \simeq \frac{3(p-2) - 2(q-2)}{16(q-p)} r. \qquad (153)$$

For $q = 2$, the above equation reduces to $n_s - 1 \simeq -3r/16$, which is valid for any $p < q$. In fact, this is the curve that gives the smallest r value for a given n_s. Unfortunately, as can be seen in Fig. 2(a), this parameter range is already excluded by observations.

In the case of $p = q$, the ϵ_U function is shown in Fig. 3 for several values of p and ξ. To the lowest order in x^{-2} we can approximate ϵ_U as

$$\epsilon_U \simeq \frac{4p^2 \xi^{2/p} x^{p-2}}{2 + 3p^2 \xi^{2/p} x^{p-2}} \cdot \frac{1}{x^4}. \qquad (154)$$

It is then clear from the above result that inflation can be realized in both regimes, for $F_{,\phi}^2 \ll F$ (i.e., $p^2 \xi^{2/p} x^{p-2} \ll 1$) and for $F_{,\phi}^2 \gg F$. The expression for ϵ_U can be simplified in both of these cases as

$$\epsilon_U \simeq \begin{cases} 2p^2 \xi^{2/p} x^{p-6} & \text{for } F_{,\phi}^2 \ll F \\ \frac{4}{3} x^{-4} & \text{for } F_{,\phi}^2 \gg F. \end{cases} \qquad (155)$$

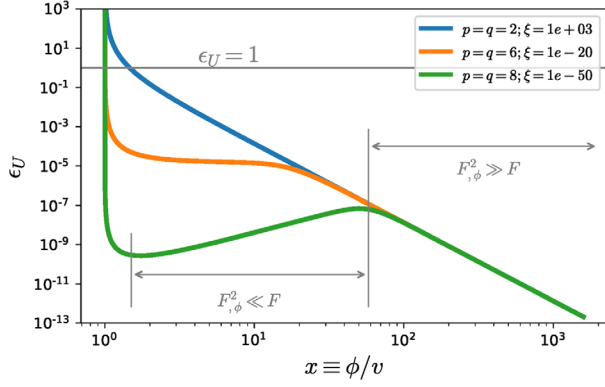Let us consider the case when cosmological scales exit the horizon in the $F_{,\phi}^2 \ll F$ regime first. Then we

FIG. 3. An illustration of the slow-roll parameter ϵ_U for chaotic type models with $p = q$. The regions that correspond to $F_{,\phi}^2 \ll F$ and $F_{,\phi}^2 \gg F$ are shown for the $p = 8$ model. ϵ_U can be approximated as in Eq. (155) in those regions.

can approximate the expression in Eq. (122) for large x values as

$$
\eta_{FV} \simeq \begin{cases} \dfrac{6-p}{2p} x^2 \epsilon_U & \text{for } p \neq 6 \\[2mm] \dfrac{1}{3} \epsilon_U & \text{for } p = 6, \end{cases} \tag{156}
$$

where we also used Eq. (155). In the case of $p = 6$ and using Eqs. (114) and (115) we find

$$
n_{\rm s} - 1 \simeq -\frac{r}{6}. \tag{157}
$$

These values also lie outside the observationally allowed region. In the case of $p \neq 6$, $\eta_{FV} \gg \epsilon_U$ and Eq. (114) is approximated by

$$
n_{\rm s} - 1 \simeq \frac{p-6}{p} x^2 \epsilon_U. \tag{158}
$$

The $1 - n_s \simeq 10^{-2}$ constraint can only be satisfied for $x \sim 1$. However, for these large values, the $x \gg 1$ condition that was used to derive Eq. (154) is violated. That is, the equations above, where the approximation $F_{,\phi}^2 \ll F$ was used, are applicable only for much smaller values of $1 - n_{\rm s}$ than what is allowed by observations.

Therefore, we are only left with the region in which the $F_{,\phi}^2 \gg F$ (i.e., $p^2 \xi^{2/p} x^{p-2} \gg 1$) approximation holds. In this limit, ϵ_U in Eq. (154) is given by

$$
\epsilon_U \simeq \frac{4}{3x^4}, \tag{159}
$$

which is independent of p. The second slow-roll parameter η_{FV}, on the other hand, can be approximated by Eq. (128). For the current model and using $x \gg 1$, this equation can be written as

$$
\eta_{FV} \simeq \frac{4}{p} \sqrt{\frac{\epsilon_U}{3}} + \frac{4}{p} \epsilon_U, \tag{160}
$$

which leads to

$$
n_{\rm s} - 1 \simeq -\frac{2}{p} \sqrt{\frac{r}{3}} - \left(\frac{4}{p} + 1\right) \frac{r}{8}. \tag{161}
$$

As we can see in Fig. 2(b), these models cross the BICEP/Keck region with $q = p$ values up to 10. However, we need to determine if this happens at the right number of e-folds before the end of inflation. To that end, we can write Eq. (116) in terms of the rescaled variable x as

$$
N \simeq \frac{1}{8\xi^{2/p} p} \int_{x_{\rm end}}^{x_*} (2 + 3p^2 \xi^{2/p} x^{p-2})(x^2 - 1) \frac{{\rm d}x^2}{x^p}, \tag{162}
$$

which can be readily integrated, leading to

$$
N_* \simeq \begin{cases} \dfrac{3}{4}\left(\dfrac{1}{6\xi} + 1\right)\left(x_*^2 - x_{\rm end}^2 + \ln \dfrac{x_{\rm end}^2}{x_*^2}\right), & \text{for } p = 2 \\[4mm] \dfrac{1}{16\xi^2}\left(x_*^{-2} - x_{\rm end}^{-2} - \ln \dfrac{x_{\rm end}^2}{x_*^2}\right) + \dfrac{3}{2}\left(x_*^2 - x_{\rm end}^2 + \ln \dfrac{x_{\rm end}^2}{x_*^2}\right), & \text{for } p = 4 \\[4mm] \dfrac{1}{2p\xi^{2/p}}\left(\dfrac{x_*^{4-p} - x_{\rm end}^{4-p}}{4-p} - \dfrac{x_*^{2-p} - x_{\rm end}^{2-p}}{2-p}\right) + \dfrac{3p}{8}\left(x_*^2 - x_{\rm end}^2 + \ln \dfrac{x_{\rm end}^2}{x_*^2}\right), & \text{otherwise.} \end{cases} \tag{163}
$$

We have already assumed that when cosmological scales exit the horizon the $F_{,\phi}^2 \gg F$ condition holds. In the case $p = 2$, this is equivalent to saying that $4\xi \gg 1$. For other values of p, this condition implies $p^2 \xi^{2/p} x_*^{p-2} \gg 1$. Thus, we can safely neglect the $(p^2 \xi^{2/p} x_*^{p-2})^{-1}$ terms, as compared to $x_*^2 \gg 1$ term or 1, from the above expression. This,

however, does not imply that we can neglect $(p^2 \xi^{2/p} x_{\rm end}^{p-2})^{-1}$ terms. In the models with $p > 2$, ξ is allowed to be small and still satisfy the $p^2 \xi^{2/p} x_*^{p-2} \gg 1$ condition, in principle.

However, as we will see shortly, in practice, observational constraints push ξ to be large and we can neglect

$(p^2 \xi^{2/p} x_{\text{end}}^{p-2})^{-1}$ terms too. Making use of $x_* \gg x_{\text{end}}$, we can eventually approximate N_* by

$$N_* \simeq \frac{3p}{8} \left(x_*^2 + \ln \frac{x_{\text{end}}^2}{x_*^2} \right). \qquad (164)$$

The logarithmic term is of the same order as the e-fold shift number in Eq. (105). Plugging that equation into the above, we find the e-fold number in the Einstein frame,

$$\hat{N}_* \simeq \frac{p}{8} \left(3x_*^2 + 5 \ln \frac{x_{\text{end}}^2}{x_*^2} \right). \qquad (165)$$

The logarithmic term can introduce a sizable correction to $\hat{N}_*$ and therefore cannot be neglected. Unfortunately, this means that we need to solve a transcendental equation for x_*, which we do numerically.

However, before solving for x_*, we need to find x_{end}. With the assumption $p^2 \xi^{2/p} \gg 1$ (or $\xi \gg p^{-p}$) it can be easily computed from Eq. (139). Plugging $q = p$ into that expression and taking $\epsilon_U|_{\text{end}} = 1$, we find

$$x_{\text{end}} \simeq \sqrt{1 + \frac{2}{\sqrt{3}}} \simeq 1.35. \qquad (166)$$

Now we can find x_* from Eq. (165) corresponding to $\hat{N}_* = 50$ and $60 e$-folds of inflation. Plugging that value into Eqs. (159)–(161), we are able to compare the results with observations. They are shown in Fig. 2(b). As we can see, practically only $p = q = 2$, 4, and 6 values are allowed.

C. Slow-roll inflation for $x \simeq 1$

So far, we have considered models for which cosmological scales exit the horizon either when $x_* \ll 1$ or $x_* \gg 1$. In this section, we look for observationally acceptable models with $x_* \simeq 1$. To that aim, let us define

$$\delta \equiv 1 - x^2, \qquad (167)$$

where $|\delta| \ll 1$.

Before doing the analysis, note that in this setup the constraints on p in Eq. (138) do not apply. Indeed, close to $x \simeq 1$ the gravitational force is always directed toward the minimum of the potential, as can be confirmed by writing

$$U_{,x} = 2U \left[-\frac{q - (q-p)\delta}{(1 - \frac{1}{2}\delta)\delta} \right]. \qquad (168)$$

For $x \lesssim 1$, δ is positive, which makes $U_{,x}$ negative and vice versa.

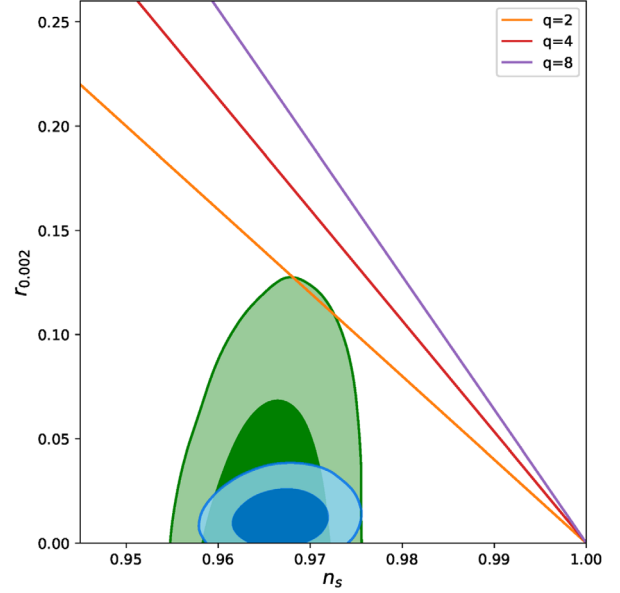Taking the first two terms in the expansion of ϵ_U in terms of δ^{-1}, we can write

FIG. 4. Comparison of observational constraints with $x_* \simeq 1$ models. The contours are the same as in Fig. 1.

$$\epsilon_U \simeq \frac{4p^2 \xi^{2/p}}{2 + 3p^2 \xi^{2/p}} \left(\frac{q}{p} \right)^2 \frac{1}{\delta^2}. \qquad (169)$$

It follows that slow-roll inflation, with $\epsilon_U \ll 1$, can be realized only for

$$p^2 \xi^{2/p} \ll 1, \qquad (170)$$

that is, $F_{,\phi}^2 \ll F$. Using this fact, the above equation for ϵ_U can be simplified as

$$\epsilon_U \simeq \frac{2q^2 \xi^{2/p}}{\delta^2}. \qquad (171)$$

Applying the same approximations to the expression of η_{FV} in Eq. (111), we get

$$\eta_{FV} \simeq \frac{4q \xi^{2/p}}{\delta^2}. \qquad (172)$$

Plugging the last two results into Eqs. (114) and (115), one finally arrives at

$$n_s - 1 \simeq -\frac{q+2}{8q} r. \qquad (173)$$

The smallest r value for a given n_s is achieved with $q = 2$. However, as can be seen in Fig. 4, even for these values the predictions lie outside the 2σ contour of the BICEP/Keck results.

Our results of Sec. V are summarized in Table I.

TABLE I. The summary of observational predictions of the generalized induced gravity inflation models in different regimes. In this table "no slow roll" signifies the absence of the $\epsilon_U \ll 1$ region. The only models that are compatible with observations are chaotic type models with $p = q \leq 6$ in the regime $F^2_{,\phi*} \gg F_*$ [see Fig. 2(b)].

		$F^2_{,\phi*} \ll F_*$	$F^2_{,\phi*} \gg F_*$
Hilltop ($x_* \ll 1$)		Eq. (145): $n_\mathrm{s} - 1 \simeq \frac{2-3p}{16p} r$	No slow roll
Chaotic ($x_* \gg 1$)	$q > p$	Eq. (153): $n_\mathrm{s} - 1 \simeq \frac{3(p-2)-2(q-2)}{16(q-p)} r$	No slow roll
	$q = p = 6$	Eq. (157): $n_\mathrm{s} - 1 \simeq -\frac{r}{6}$	Eq. (161): $n_\mathrm{s} - 1 \simeq -\frac{2}{p}\sqrt{\frac{r}{3}} - (\frac{4}{p}+1)\frac{r}{8}$
	$q = p \neq 6$	Eq. (158): $n_\mathrm{s} - 1 \simeq \frac{p-6}{p} x_*^2 \epsilon_U$	
$x_* \simeq 1$		Eq. (173): $n_\mathrm{s} - 1 \simeq -\frac{q+2}{8q} r$	No slow roll

VI. SUMMARY AND CONCLUSIONS

In this work, we consider inflation models within the framework of scalar-tensor theories of gravity. The most straightforward way to analyze such models and confront them with observations is to transform the action into the Einstein frame. However, this is not always desirable. For example, after the transformation, the matter sector directly couples to the scalar field, even if no such coupling is introduced in the Jordan frame. For certain applications, this might actually complicate the analysis. In those cases, it would be convenient to have a formalism where inflation observables can be calculated only relying on Jordan frame quantities. In this work, we derive the requirements that Jordan frame quantities must satisfy to provide slow-roll inflation. We also derive Jordan frame flow and slow-roll parameters, which must be small, and write inflation observables in terms of those parameters.

The central idea of our method is to utilize the fact that conformal transformation corresponds to the change of units of measure [45]. We assume to slice the spacetime into spacelike hypersurfaces and keep that slicing fixed. It allows us to map the relations defined in the Einstein frame to the Jordan frame on the same slice by changing the units of measure (performing the conformal transformation). In particular, we take the conditions required for inflation and more stringent conditions for slow-roll inflation, which are most clearly defined in the Einstein frame, and map them to the Jordan frame.

We also make use of another convenient fact that the scalar and tensor metric perturbation spectra in single field slow-roll inflation models can be conveniently written in terms of homogeneous quantities only. Hence, only the homogeneous relations need to be mapped from the Einstein to the Jordan frame in order to derive observable model predictions.

Using this method, we first derive the conditions for inflation. It has been noted in various places in the literature (see, e.g., [10]) that those conditions in the Jordan frame might look somewhat counterintuitive from the Einstein frame perspective. For example, the Jordan frame scale factor does not have to be accelerating, as was demonstrated in Eq. (73), or the Hubble-flow parameter ϵ_1 does not have to be smaller than 1 [see Eq. (71)]. This has to be kept in mind when doing computations that are related to the end of inflation.

However, once we impose a much stronger requirement, that the Einstein frame Hubble-flow parameter $\hat{\epsilon}_1 \ll 1$ [see Eq. (6) for the definition], the conditions become more stringent. In that case, some of the familiar expressions in the Einstein frame can be carried over to the Jordan one. In particular, Eqs. (78) and (86), which for convenience we rewrite here, are

$$\frac{1}{2}\dot{\phi}^2 \ll V,$$

$$\frac{\dot{V}}{HV} \ll 1.$$

In the Jordan frame, we have an additional function F, which enlarges the number of conditions. To find a compact parametrization for them, we introduced a number of flow parameters, in analogy to the Hubble-flow parameters. These are ϵ_i, θ_i, and γ^2 defined in Eqs. (65)–(67). We demonstrated in this work that the requirement $\hat{\epsilon}_i \ll 1$ translates into the Jordan frame as

$$\epsilon_1, \gamma^2, |\gamma_2|, |\theta_1|, |\theta_1\theta_2| \ll 1.$$

The above relations are derived in Eqs. (89), (92), (88), (82), and (95), respectively.

Only two of the three sets of parameters ϵ_i, θ_i, and γ_i are needed to describe the system, and we found that using θ_i and γ_i results in the most compact equations. However, when computing inflation observables, we provide two combinations. In Eqs. (96)–(98) the scalar spectral index, scalar spectral tilt, and tensor-to-scalar ratio, A_s, n_s, and r, respectively, are written as functions of γ_i and θ_i,

$$A_\mathrm{s} \simeq \frac{V}{24\pi^2 F^2 \gamma^2},$$

$$n_\mathrm{s} - 1 \simeq -2(\gamma^2 + \gamma_2 - \theta_1\theta_2),$$

$$r \simeq 16\gamma^2.$$

And in Eqs. (100)–(102), they are written as functions of ϵ_i and θ_i.

We also derive the slow-roll equations in the Jordan frame. As described above, we take the Einstein frame version of slow-roll conditions in Eqs. (47) and (48) and after the conformal transformation they can be written as in Eqs. (74) and (76). Taking into account all the smallness conditions discussed above, we finally arrive at Eqs. (83) and (85),

$$H^2 \simeq \frac{V}{3F},$$
$$3H\dot{\phi} \simeq \frac{2VF_{,\phi} - FV_{,\phi}}{F^2 \mathcal{K}},$$

which are the Jordan frame versions of the slow-roll Friedman equation and equation of motion. These approximate relations can be applied as long as slow-roll conditions $\epsilon_U, |\eta_{FV}| \ll 1$ are satisfied, where the slow-roll parameters are defined in Eqs. (109) and (111),

$$\epsilon_U = \frac{1}{2\mathcal{K}} \left(\frac{V_{,\phi}}{V} - 2\frac{F_{,\phi}}{F} \right)^2,$$
$$\eta_{FV} = \frac{1}{\mathcal{K}} \left[2\frac{F_{,\phi\phi}}{F} - \frac{V_{,\phi\phi}}{V} - 2\frac{F_{,\phi}^2}{F^2} + \frac{V_{,\phi}^2}{V^2} + \frac{\mathcal{K}_{,\phi}}{2\mathcal{K}} \left(\frac{V_{,\phi}}{V} - 2\frac{F_{,\phi}}{F} \right) \right],$$

where ϵ_U is the same slow-roll parameter as in the Einstein frame but expressed in terms of the Jordan frame quantities. The dependence of inflation observables on ϵ_U and η_{FV} is given in Eqs. (113)–(115),

$$A_s \simeq \frac{V}{24\pi^2 F^2 \epsilon_U},$$
$$n_s - 1 \simeq -2(\epsilon_U + \eta_{FV}),$$
$$r \simeq 16\epsilon_U.$$

When computing numerical values of the above parameters, another aspect that has to be taken into account is the difference between the number of e-folds of inflation as defined with respect to $\hat{a}$ and a, i.e., the scale factors in the Einstein and Jordan frames, respectively. This difference is proportional to the logarithm of F, as shown in Eq. (105),

$$\hat{N} = N + \frac{1}{2} \ln \frac{F_{\text{end}}}{F}.$$

Although the e-fold shift number $\ln \sqrt{F_{\text{end}}/F}$ is logarithmic, it can be substantial and therefore generically cannot be neglected, as we demonstrate in the case of induced gravity models of inflation. When comparing with observations, we used $\hat{N}$ from 50 to 60, which are the values used by the Planck team.

Finally, we should also mention another known fact, that in the Jordan frame the field does not necessarily roll down the potential $V(\phi)$ even in slow roll. As the strength and the direction of the gravitational force depends on $F(\phi)$, the field ϕ can as well climb up that potential. This can be readily understood by looking at the gradient of the scalar field potential in the Einstein frame in Eq. (64). The direction of the gravitational force is no longer determined solely by the gradient of $V(\phi)$, but in combination with the gradient of $F(\phi)$. This has to be taken into account when considering models of inflation, as we also demonstrate in our example model in Sec. V.

In that section, we consider a generalized induced gravity model. The main idea of induced gravity theories is to generate gravity by a spontaneous symmetry breaking [66–69]. That is, general relativity is recovered after the ϕ field settles at its vacuum expectation value, which is determined by the potential $V(\phi)$. To make sure that the field slowly rolls toward the minimum of $V(\phi)$ one needs to constrain possible functional forms of $F(\phi)$.

The main goal of Sec. V is to apply some of our results to a concrete model. Making use of Jordan frame quantities only, we analyze the model specified in Eqs. (131) and (132) and look for observationally acceptable parameter space. We found that, among the many regions where slow-roll inflation could be realized, only the case with $p = q = 2$, 4, and 6 in the chaotic type regime (where $|\phi_*| \gg |v|$) falls within 2σ region of the newest BICEP/Keck results [65] [see Fig. 2(b)].

Finally, to validate our method, we performed numerical simulations in which we solved exact perturbation equations in the Einstein frame and compared them with our Jordan frame slow-roll approximations. As can be seen in the Appendix and Fig. 2(b), the agreement is very good indeed.

In this work, we neglected a possible contribution from matter fields to the dynamics of the system. We also analyzed single field models only. These simplifications allowed a simple check of the above results by transforming the action into the Einstein frame and performing exact computations numerically. In the future, we plan to extend our formalism by including those complications, such as matter fields and considering multifield models, which will bring us closer to the real motivation of this work.

ACKNOWLEDGMENTS

APPENDIX: COMPARISON OF FLOW PARAMETERS WITH NUMERICAL SIMULATIONS

To see how well our approximations perform, we compared them with exact numerical solutions. To that

purpose, we used the induced gravity model in Eqs. (131) and (132) with $p = q = 2$ and $\phi_*/v \gg 1$. As shown in Fig. 2(b), this model conforms to observations very well.

The numerical simulations are performed in both frames. In the case of the Einstein frame, we first transform the Jordan frame action in Eq. (53) using the conformal transformation in Eq. (16). This results in a scalar field with a noncanonical kinetic function as in Eq. (25) and background equations (26), (30), and (31). Using Eq. (51), they can be also expressed in terms of the number of e-folds $\hat{N}$,

$$\frac{d^2\phi}{d\hat{N}^2} - \left(3 - \frac{1}{\hat{H}}\frac{d\hat{H}}{d\hat{N}}\right)\frac{d\phi}{d\hat{N}} + \frac{1}{2}\frac{\mathcal{K}_{,\phi}}{\mathcal{K}}\left(\frac{d\phi}{d\hat{N}}\right)^2 + \frac{U_{,\phi}}{\mathcal{K}\hat{H}^2} = 0,$$
$$(A1)$$

$$\hat{H}^2 = \frac{U(\phi)}{3 - \frac{1}{2}\mathcal{K}(\frac{d\phi}{d\hat{N}})^2},$$
$$(A2)$$

$$\frac{d\hat{H}}{d\hat{N}} = \frac{1}{2}\mathcal{K}\hat{H}\left(\frac{d\phi}{d\hat{N}}\right)^2,$$
$$(A3)$$

where the kinetic term is given by

$$\mathcal{K} = \left(\frac{1}{\xi} + 6\right)\frac{1}{\phi^2},$$
$$(A4)$$

and the lapse function $\hat{\mathcal{N}} = \sqrt{F} = \sqrt{\xi}\phi$.

Alongside homogeneous equations, we also integrate equations for perturbations. The curvature perturbation $\hat{\mathcal{R}}_k$ is related to the field perturbations $\delta\phi_k$ by [21]

$$\hat{\mathcal{R}}_k = -\frac{\hat{u}_k}{\hat{a}\frac{d\phi}{d\hat{N}}\sqrt{\mathcal{K}}},$$
$$(A5)$$

where $\hat{u}_k \equiv \hat{a}\sqrt{\mathcal{K}}\delta\phi_k$ is the Mukhanov-Sasaki variable. The evolution of $\hat{\mathcal{R}}_k$ is governed by the equation

$$\ddot{\hat{\mathcal{R}}}_k + \left[(3 + \hat{\epsilon}_2)\sqrt{F} - \frac{1}{2}\frac{\dot{F}}{\hat{H}F}\right]\hat{H}\dot{\hat{\mathcal{R}}}_k + F\frac{k^2}{\hat{a}^2}\hat{\mathcal{R}}_k = 0. \quad (A6)$$

In terms of the number of e-folds, it can be written as

$$\frac{d^2\hat{\mathcal{R}}_k}{d\hat{N}^2} - (3 - \hat{\epsilon}_1 + \hat{\epsilon}_2)\frac{d\hat{\mathcal{R}}_k}{d\hat{N}} + \frac{k^2}{\hat{a}^2\hat{H}^2}\hat{\mathcal{R}}_k = 0, \quad (A7)$$

where the Hubble-flow parameters $\hat{\epsilon}_i$ are defined in Eq. (6). The above equation is solved starting from Bunch-Davies vacuum initial conditions,

$$\hat{u}_{k,\text{vac}} = \frac{1}{\sqrt{2k}}e^{ik/(\hat{a}\hat{H})},$$
$$(A8)$$

$\hat{N} = 5$ e-folds before the horizon exit, which is defined as $k = \hat{a}\hat{H}$, until $\hat{N} = 5$ e-folds after the horizon exit. The

latter five e-folds are added in order to make it certain that the decaying mode is negligible and $\hat{\mathcal{R}}_k$ remains constant afterward, whereas we start integrating five e-folds before horizon-crossing time to ensure that $k/(\hat{a}\hat{H}) \gg 1$, so Eq. (A8) is a good approximation for the field perturbations.

The power spectrum of $\hat{\mathcal{R}}$ and the spectral tilt are computed using

$$A_s = \frac{k^3}{2\pi^2}|\hat{\mathcal{R}}_k|^2,$$
$$(A9)$$

and

$$n_s - 1 = \frac{d \ln A_s}{d \ln k}.$$
$$(A10)$$

Similarly, we compute the amplitude of tensor perturbations. In terms of the number of $\hat{N}$ e-folds, it is given by

$$\frac{d^2\hat{h}_k}{d\hat{N}^2} - (3 - \hat{\epsilon}_1)\frac{d\hat{h}_k}{d\hat{N}} + \frac{k^2}{\hat{a}^2\hat{H}^2}\hat{h}_k = 0, \quad (A11)$$

with initial conditions

$$\hat{h}_{k,\text{vac}} = 2\frac{\hat{u}_{k,\text{vac}}}{\hat{a}}.$$
$$(A12)$$

The tensor-to-scalar ratio is given by

$$r \equiv \frac{A_t}{A_s},$$
$$(A13)$$

where the tensor amplitude is defined by

$$A_t = \frac{k^3}{2\pi^2}|\hat{h}_k|^2.$$
$$(A14)$$

As we integrate Eqs. (A1)–(A3), (A7), and (A11), we also compute the coordinate time using Eq. (51),

$$t_{\text{end}} - t = \int_0^{\hat{N}} \frac{d\hat{N}}{\sqrt{F}\hat{H}},$$
$$(A15)$$

where $t_{\text{end}} > t$ and t_{end} is an arbitrary value at the end of inflation.

In the Jordan frame, we only need to integrate homogeneous equations. To make sure we start from the same spatial slice, the initial values of ϕ and $\dot{\phi}$ are taken exactly the same as in the simulations above. Then, using definitions of $\hat{N}$ and N in Eqs. (51) and (103) together with Eqs. (59) and (60), we can relate the derivatives in both frames by

$$\frac{d\phi}{dN} = \frac{1}{1 + \frac{F_{,\phi}}{2F}\frac{d\phi}{d\hat{N}}}\frac{d\phi}{d\hat{N}}.$$
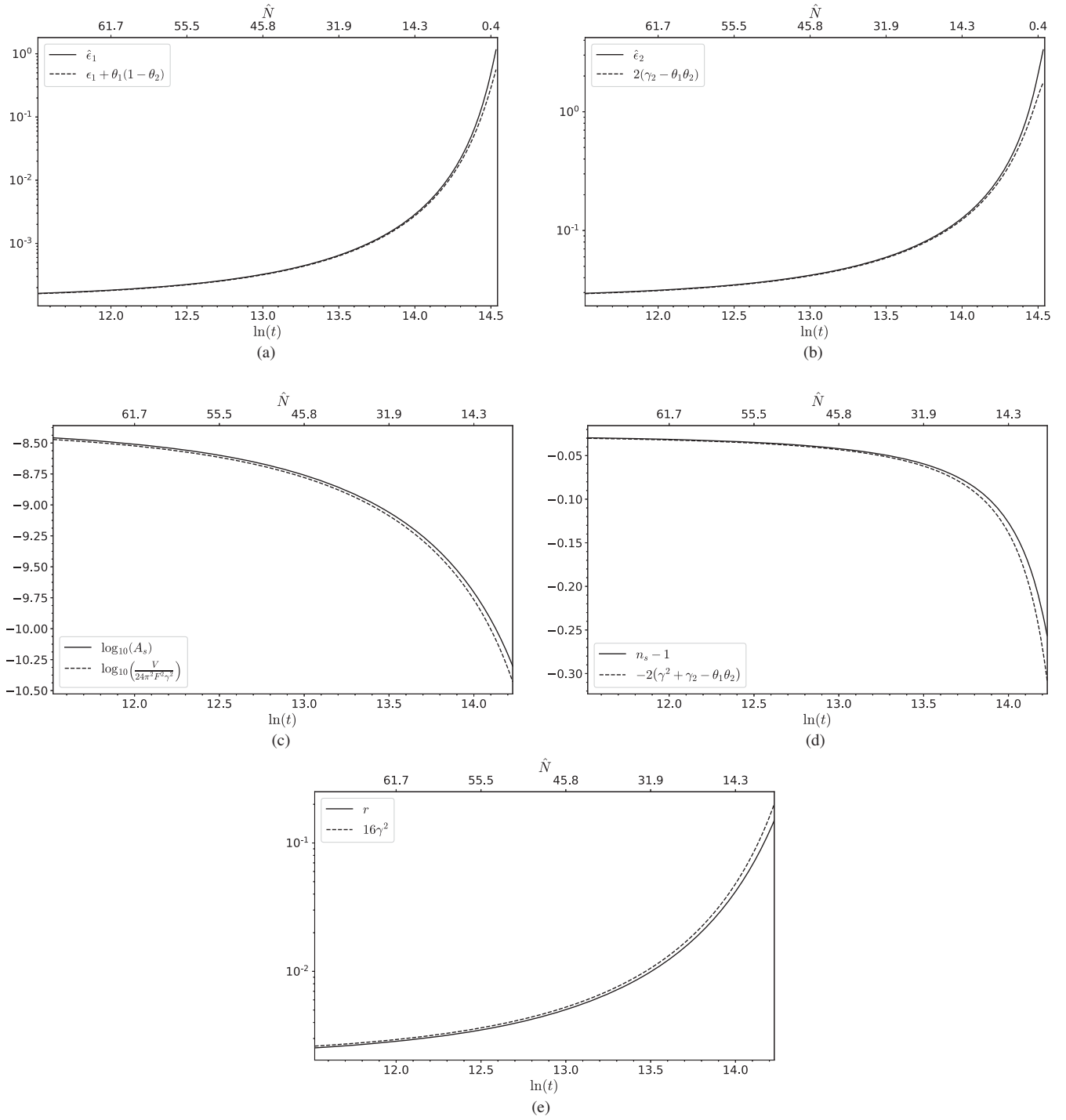$$(A16)$$

FIG. 5. The comparison of exact, numerical Einstein frame results and approximate relations derived in this work. We used the model defined in Eqs. (131) and (132) with $p = q = 2$. These functions are plotted against the time t, which enumerates spatial slices and are shown on the lower horizontal axis. The upper horizontal axis shows the corresponding e-fold number $\hat{N}(t)$ in the Einstein frame for the reference. (a) Numerical check of Eq. (107), where γ is approximated by Eq. (99). (b)–(e) Numerical check of Eqs. (94), (96), (97), and (98), respectively.

The homogeneous system of Jordan frame equations that we are solving are given in Eqs. (61)–(63). In terms of e-fold numbers N, they can be written as

$$\frac{d^2\phi}{dN^2} - (3 - \epsilon_1)\frac{d\phi}{dN} + \frac{V_{,\phi}}{H^2} = 3F_{,\phi}(2 - \epsilon_1), \qquad \text{(A17)}$$

$$H^2 = \frac{V}{3F}\frac{1}{1 - \frac{1}{6F}\left(\frac{d\phi}{dN}\right)^2 + 2\theta_1}, \qquad \text{(A18)}$$

$$\epsilon_1 = -\frac{\left(\frac{d\phi}{dN}\right)^2 + \frac{dF}{dN} + \frac{d^2F}{dN^2}}{2F(1 + \theta_1)}, \qquad \text{(A19)}$$

where θ_1 is defined in Eq. (66). The coordinate time is calculated by integrating [cf. Eq. (103)]

$$t_{\text{end}} - t = \int_0^N \frac{dN}{H}. \qquad \text{(A20)}$$

Having computed the time variable t in both frames, we can compare the results from the Jordan and Einstein frames on the same time slice. The results are shown in Fig. 5. In that figure, we compare the exact Einstein frame calculations with the corresponding Jordan frame slow-roll approximations. In particular, in Figs. 5(a) and 5(b), we see that the agreement between the first two Einstein frame Hubble-flow parameters and their expressions in terms of
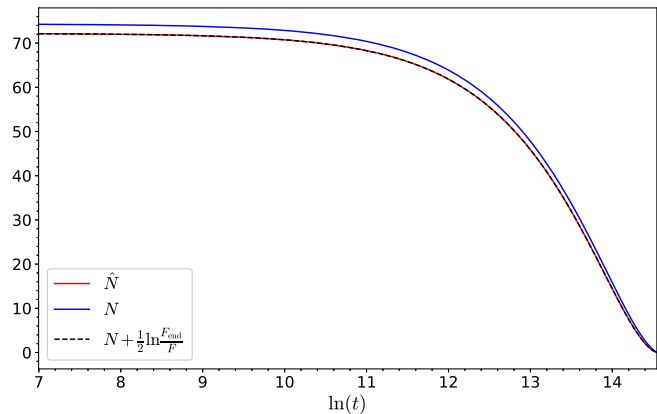

FIG. 6. The e-fold number in each frame after solving numerically the exact field equations. We show the effect of the e-fold shift number as in Eq. (105).

Jordan frame flow parameters agree very well. While looking at Figs. 5(c)–5(e), we can conclude the same about the exact simulations of inflation observables and their approximate expressions in terms of Jordan frame flow parameters.

We can also check numerically the exact relation between $\hat{N}$ and N in Eq. (105). We plot their values on the same spatial slice in Fig. 6. As one can see, adding the e-fold shift number makes both curves $\hat{N}(t)$ and $N(t)$ overlap exactly.

[1] A. A. Starobinsky, A new type of isotropic cosmological models without singularity, Phys. Lett. **91B**, 99 (1980).

[2] D. La and P. J. Steinhardt, Extended Inflationary Cosmology, Phys. Rev. Lett. **62**, 376 (1989).

[3] J. McDonald, Chaotic inflation in Brans-Dicke models, Phys. Rev. D **44**, 2314 (1991).

[4] P. J. Steinhardt and F. S. Accetta, Hyperextended Inflation, Phys. Rev. Lett. **64**, 2740 (1990).

[5] B. Spokoiny, Inflation and generation of perturbations in broken-symmetric theory of gravity, Phys. Lett. **147B**, 39 (1984).

[6] F. S. Accetta, D. J. Zoller, and M. S. Turner, Induced gravity inflation, Phys. Rev. D **31**, 3046 (1985).

[7] F. Lucchin, S. Matarrese, and M. D. Pollock, Inflation with a nonminimally coupled scalar field, Phys. Lett. **167B**, 163 (1986).

[8] F. L. Bezrukov and M. Shaposhnikov, The standard model Higgs boson as the inflaton, Phys. Lett. B **659**, 703 (2008).

[9] D. H. Coule, Pre-big bang model has Planck problem, Classical Quantum Gravity **15**, 2803 (1998).

[10] V. Faraoni, Cosmology in Scalar Tensor Gravity, 1st ed. (Springer, Dordrecht, 2004).

[11] D. Lyth and A. Liddle, The Primordial Density Perturbation: Cosmology, Inflation and the Origin of Structure (Cambridge University Press, Cambridge, England, 2009).

[12] E. D. Stewart and D. H. Lyth, A more accurate analytic calculation of the spectrum of cosmological perturbations produced during inflation, Phys. Lett. B **302**, 171 (1993).

[13] J.-O. Gong and E. D. Stewart, The density perturbation power spectrum to second order corrections in the slow roll expansion, Phys. Lett. B **510**, 1 (2001).

[14] S. M. Leach, A. R. Liddle, J. Martin, and D. J. Schwarz, Cosmological parameter estimation and the inflationary cosmology, Phys. Rev. D **66**, 023515 (2002).

[15] Planck Collaboration, Planck 2018 results. X. Constraints on inflation, Astron. Astrophys. **641**, A10 (2020).

[16] Planck Collaboration, Planck 2013 results. XXII. Constraints on inflation, Astron. Astrophys. **571**, A22 (2014).

[17] V. Domcke and K. Schmitz, Inflation from high-scale supersymmetry breaking, Phys. Rev. D **97**, 115025 (2018).

[18] P. Kuusk, M. Rünkla, M. Saal, and O. Vilson, Invariant slow-roll parameters in scalar-tensor theories, Classical Quantum Gravity **33**, 195008 (2016).

[19] J. C. Hwang, Cosmological perturbations in generalized gravity theories: Formulation, Classical Quantum Gravity 7, 1613 (1990).

[20] J. C. Hwang, Cosmological perturbations in generalized gravity theories: Solutions, Phys. Rev. D 42, 2601 (1990).

[21] J.-c. Hwang and H. Noh, Cosmological perturbations in generalized gravity theories, Phys. Rev. D 54, 1460 (1996).

[22] R. Myrzakulov, L. Sebastiani, and S. Vagnozzi, Inflation in $f(R, \phi)$-theories and mimetic gravity scenario, Eur. Phys. J. C 75, 444 (2015).

[23] E. Elizalde, S. D. Odintsov, V. K. Oikonomou, and T. Paul, Logarithmic-corrected R^2 gravity inflation in the presence of Kalb-Ramond fields, J. Cosmol. Astropart. Phys. 02 (2019) 017.

[24] R. Fakir, Quantum creation of universes with nonminimal coupling, Phys. Rev. D 41, 3012 (1990).

[25] N. Makino and M. Sasaki, The density perturbation in the chaotic inflation with nonminimal coupling, Prog. Theor. Phys. 86, 103 (1991).

[26] J.-O. Gong, J.-c. Hwang, W.-I. Park, M. Sasaki, and Y.-S. Song, Conformal invariance of curvature perturbation, J. Cosmol. Astropart. Phys. 09 (2011) 023.

[27] J. White, M. Minamitsuji, and M. Sasaki, Curvature perturbation in multi-field inflation with non-minimal coupling, J. Cosmol. Astropart. Phys. 07 (2012) 039.

[28] T. Kubota, N. Misumi, W. Naylor, and N. Okuda, The conformal transformation in general single field inflation with non-minimal coupling, J. Cosmol. Astropart. Phys. 02 (2012) 034.

[29] R. Catena, M. Pietroni, and L. Scarabello, Einstein and Jordan reconciled: A frame-invariant approach to scalar-tensor cosmology, Phys. Rev. D 76, 084039 (2007).

[30] R. Catena, M. Pietroni, and L. Scarabello, Local transformations of units in scalar-tensor cosmology, J. Phys. A 40, 6883 (2007).

[31] A. Racioppi and M. Vasar, On the number of e-folds in the Jordan and Einstein frames, Eur. Phys. J. Plus 137, 637 (2022).

[32] D. I. Kaiser, Frame independent calculation of spectral indices from inflation, arXiv:astro-ph/9507048.

[33] T. Prokopec and J. Weenink, Frame independent cosmological perturbations, J. Cosmol. Astropart. Phys. 09 (2013) 027.

[34] L. Järv, K. Kannike, L. Marzola, A. Racioppi, M. Raidal, M. Rünkla, M. Saal, and H. Veermäe, Frame-Independent Classification of Single-Field Inflationary Models, Phys. Rev. Lett. 118, 151302 (2017).

[35] J. Garcia-Bellido, A. D. Linde, and D. A. Linde, Fluctuations of the gravitational constant in the inflationary Brans-Dicke cosmology, Phys. Rev. D 50, 730 (1994).

[36] D. F. Torres, Slow roll inflation in nonminimally coupled theories: Hyperextended gravity approach, Phys. Lett. A 225, 13 (1997).

[37] J. R. Morris, Generalized slow roll conditions and the possibility of intermediate scale inflation in scalar tensor theory, Classical Quantum Gravity 18, 2977 (2001).

[38] T. Chiba and M. Yamaguchi, Extended slow-roll conditions and rapid-roll conditions, J. Cosmol. Astropart. Phys. 10 (2008) 021.

[39] K. Akın, A. Savaş Arapoglu, and A. Emrah Yükselci, Formalizing slow-roll inflation in scalar-tensor theories of gravitation, Phys. Dark Universe 30, 100691 (2020).

[40] L. Järv and A. Toporensky, Global portraits of nonminimal inflation, Eur. Phys. J. C 82, 179 (2022).

[41] E. E. Flanagan, The conformal frame freedom in theories of gravitation, Classical Quantum Gravity 21, 3817 (2004).

[42] V. Faraoni and S. Nadeau, The (pseudo)issue of the conformal frame revisited, Phys. Rev. D 75, 023501 (2007).

[43] H. Azri, Are there really conformal frames? Uniqueness of affine inflation, Int. J. Mod. Phys. D 27, 1830006 (2018).

[44] E. Gourgoulhon, $3 + 1$ formalism and bases of numerical relativity, arXiv:gr-qc/0703035.

[45] R. Dicke, Mach's principle and invariance under transformation of units, Phys. Rev. 125, 2163 (1962).

[46] N. D. Birrell and P. C. W. Davies, *Quantum Fields in Curved Space*, Cambridge Monographs on Mathematical Physics (Cambridge University Press, Cambridge, England, 1984).

[47] N. Deruelle and M. Sasaki, Conformal equivalence in classical gravity: The example of 'veiled' general relativity, Springer Proc. Phys. 137, 247 (2011).

[48] G. Domènech and M. Sasaki, Conformal frames in cosmology, Int. J. Mod. Phys. D 25, 1645006 (2016).

[49] E. Poisson, *A Relativist's Toolkit: The Mathematics of Black-Hole Mechanics* (Cambridge University Press, Cambridge, England, 2009).

[50] M. Fierz, On the physical interpretation of P. Jordan's extended theory of gravitation, Helv. Phys. Acta 29, 128 (1956).

[51] C. Brans and R. H. Dicke, Mach's principle and a relativistic theory of gravitation, Phys. Rev. 124, 925 (1961).

[52] T. Kodama and T. Takahashi, Relaxing inflation models with nonminimal coupling: A general study, Phys. Rev. D 105, 063542 (2022).

[53] V. Faraoni, Generalized slow roll inflation, Phys. Lett. A 269, 209 (2000).

[54] A. Karam, T. Pappas, and K. Tamvakis, Frame-dependence of higher-order inflationary observables in scalar-tensor theories, Phys. Rev. D 96, 064036 (2017).

[55] R. N. Lerner and J. McDonald, Higgs inflation and naturalness, J. Cosmol. Astropart. Phys. 04 (2010) 015.

[56] T. Futamase and K.-i. Maeda, Chaotic inflationary scenario in models having nonminimal coupling with curvature, Phys. Rev. D 39, 399 (1989).

[57] S. C. Hyun, J. Kim, S. C. Park, and T. Takahashi, Non-minimally assisted chaotic inflation, J. Cosmol. Astropart. Phys. 05 (2022) 045.

[58] M. D. Pollock and D. Sahdev, Pole law inflation in a theory of induced gravity, Phys. Lett. B 222, 12 (1989).

[59] D. I. Kaiser, Constraints in the context of induced gravity inflation, Phys. Rev. D 49, 6347 (1994).

[60] J. L. Cervantes-Cota and H. Dehnen, Induced gravity inflation in the SU(5) GUT, Phys. Rev. D 51, 395 (1995).

[61] R. Fakir and W. G. Unruh, Induced gravity inflation, Phys. Rev. D **41,** 1792 (1990).

[62] D. S. Salopek, J. R. Bond, and J. M. Bardeen, Designing density fluctuation spectra in inflation, Phys. Rev. D **40,** 1753 (1989).

[63] D. I. Kaiser, Induced gravity inflation and the density perturbation spectrum, Phys. Lett. B **340,** 23 (1994).

[64] D. I. Kaiser, Primordial spectral indices from generalized Einstein theories, Phys. Rev. D **52,** 4295 (1995).

[65] BICEP and Keck Collaboration, Improved Constraints on Primordial Gravitational Waves using Planck, WMAP, and BICEP/Keck Observations through the 2018 Observing Season, Phys. Rev. Lett. **127,** 151301 (2021).

[66] A. D. Sakharov, Vacuum quantum fluctuations in curved space and the theory of gravitation, Dokl. Akad. Nauk Ser. Fiz. **177,** 70 (1967).

[67] J. O'Hanlon, Intermediate-Range Gravity: A Generally Covariant Model, Phys. Rev. Lett. **29,** 137 (1972).

[68] A. Zee, A Broken Symmetry Theory of Gravity, Phys. Rev. Lett. **42,** 417 (1979).

[69] L. Smolin, Towards a theory of space-time structure at very short distances, Nucl. Phys. **B160,** 253 (1979).